Provided for non-commercial research and education use.
Not for reproduction, distribution or commercial use.

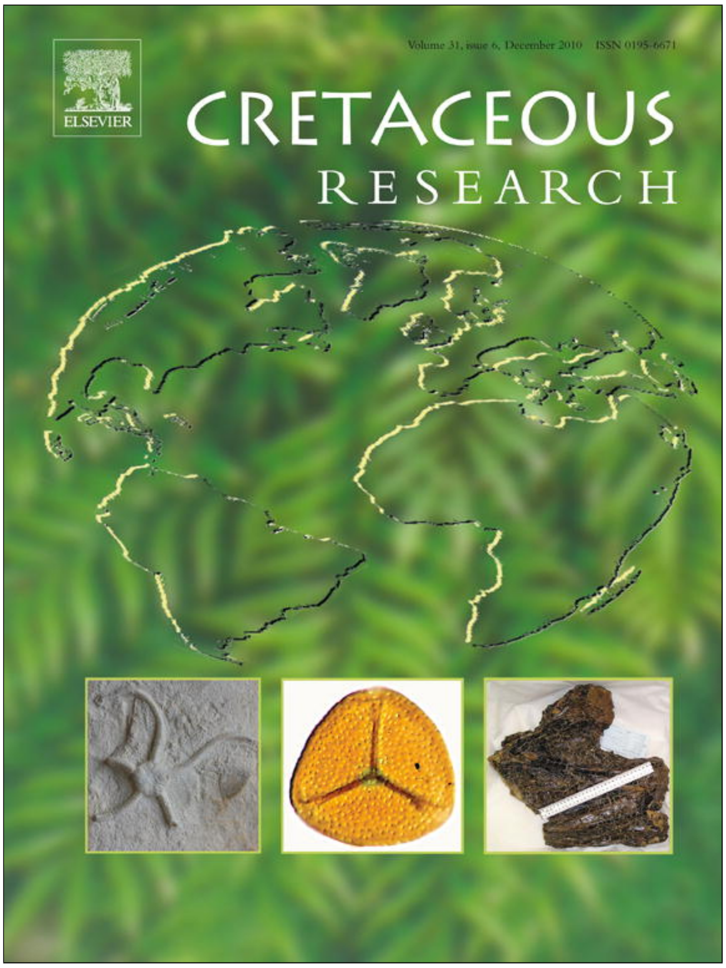

This article appeared in a journal published by Elsevier. The attached copy is furnished to the author for internal non-commercial research and education use, including for instruction at the authors institution and sharing with colleagues.

Other uses, including reproduction and distribution, or selling or licensing copies, or posting to personal, institutional or third party websites are prohibited.

In most cases authors are permitted to post their version of the article (e.g. in Word or Tex form) to their personal website or institutional repository. Authors requiring further information regarding Elsevier's archiving and manuscript policies are encouraged to visit:

http://www.elsevier.com/copyright

Author's personal copy

Cretaceous Research 31 (2010) 577–592

Contents lists available at ScienceDirect

Cretaceous Research

journal homepage: www.elsevier.com/locate/CretRes

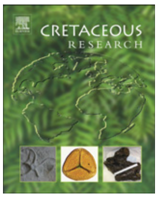

The Valanginian positive carbon isotope event in Arctic Russia: Evidence from terrestrial and marine isotope records and implications for global carbon cycling

Elizabeth V. Nunn[a,b,*], Gregory D. Price[a], Darren R. Gröcke[c], Evgenij Y. Baraboshkin[d], Melanie J. Leng[e], Malcolm B. Hart[a]

[a] *School of Geography, Earth and Environmental Sciences, University of Plymouth, Drake Circus, Plymouth, PL4 8AA, UK*
[b] *Earth System Science Research Centre, Department of Applied and Analytical Paleontology, Institute of Geosciences, University of Mainz, Johann-Joachim-Becher-Weg 21, 55128 Mainz, Germany*
[c] *Department of Earth Sciences, Durham University, Science Laboratories, South Road, Durham DH1 3LE, UK*
[d] *Department of Regional Geology and Earth History, Geological Faculty, Moscow State University, Vorobjovy Gory, 119991 Moscow, Russia*
[e] *NERC Isotope Geosciences Laboratory, British Geological Survey, Kingsley Dunham Centre, Keyworth, Nottingham NG12 5GG, UK*

ARTICLE INFO

Article history:
Received 4 December 2009
Accepted in revised form 23 July 2010
Available online 30 July 2010

Keywords:
Carbon isotopes
Russia
Valanginian
Wood
Belemnites

ABSTRACT

The data presented here comprise Ryazanian–Valanginian carbon isotope ratios analyzed from fossil wood and belemnites from the shallow marine Boyarka River succession in Siberia. Additional belemnite carbon isotope ratios from the Izhma River succession (also Ryazanian–Valanginian) in Russia are also presented. The wood-derived and belemnite-derived isotope ratios are considered to primarily reflect changes in the terrestrial and marine carbon isotope reservoirs respectively. The $\delta^{13}C_{carb}$ and $\delta^{13}C_{wood}$ records reveal a distinct mid-Valanginian positive carbon isotope excursion, with the initiation occurring near the Boreal Russian *michalskii–polyptychus* zone boundary, which is broadly time-equivalent Tethyan *campylotoxus –verrucosum* boundary. The Ryazanian–Valanginian $\delta^{13}C_{carb}$ values fluctuate between c. −1 and +1.5‰ but reach a maximum of +4.1‰ in the Late Valanginian, whilst the $\delta^{13}C_{wood}$ values fluctuate between c. −27 and −23.5‰ and reach a Late Valanginian maximum of −21.2‰. The excursion maximum in the Boreal Russian *bidichotomus* zones corresponds with the peak of the Tethyan marine carbonate excursion in the *verrucosum–peregrinus* zones, the peak of a marine carbonate excursion recorded in the Argentinean *atherstoni* Zone and also with the peak of a terrestrial organic carbon isotope excursion in the Crimean *trinodosum–callidiscus* ammonite zones. The synchroneity of the positive carbon isotope event between the marine and terrestrial records and between the northern and southern hemispheres and Tethys, clearly indicates a strong coupling of the ocean–atmosphere system at this time and also confirms that this was a global event, which would have affected the total exchangeable carbon reservoir.

© 2010 Elsevier Ltd. All rights reserved.

1. Introduction

The mid-Valanginian positive carbon isotope event is well known in marine carbonates. It has been linked to Cretaceous greenhouse conditions (e.g., Lini et al., 1992), related to eruption of the Paraná–Etendeka continental flood basalts (e.g., Channell et al., 1993; Courtillot et al., 1999; Erba et al., 2004; Gröcke et al., 2005) and to the drowning of carbonate-platforms along the Northern Tethyan margin (e.g., Föllmi et al., 1994). Positive carbon isotope excursions are typically attributed to increased productivity and/or enhanced preservation of organic matter, for example, as black shales. Both processes effectively increase the amount of ^{12}C locked out of the global carbon cycle and therefore, enrich the global $\delta^{13}C$ signal with the heavier isotope ^{13}C. What is particularly interesting about the Valanginian is the apparent absence of widespread marine black shales, although, a few isolated occurrences of Valanginian marine organic matter have been identified, for example at DSDP Site 535 in the Straits of Florida (Herbin et al., 1984) and more recently on the Shatsky Rise (ODP Leg 198, Site 1213; Shipboard Scientific Party, 2002; Westermann et al., 2010). A number of other DSDP and ODP sites have recorded Valanginian organic-rich horizons in the Atlantic, for example Sites 416 and 638, however the organic matter in these horizons is typically terrestrial

---

[*] Corresponding author. Earth System Science Research Centre, Department of Applied and Analytical Paleontology, Institute of Geosciences, University of Mainz, Johann-Joachim-Becher-Weg 21, 55128 Mainz, Germany. Tel.: +49 (0) 6131 39 22387; fax: +49 (0) 6131 39 24768.

E-mail addresses: nunn@uni-mainz.de (E.V. Nunn), G.Price@plymouth.ac.uk (G.D. Price), d.r.grocke@durham.ac.uk (D.R. Gröcke), Barabosh@geol.msu.ru (E.Y. Baraboshkin), mjl@bgs.ac.uk (M.J. Leng), M.Hart@plymouth.ac.uk (M.B. Hart).

0195-6671/$ – see front matter © 2010 Elsevier Ltd. All rights reserved.
doi:10.1016/j.cretres.2010.07.007

Author's personal copy

in origin (e.g., Claypool and Baysinger, 1980). Several other carbon isotope investigations have shown that the deposition of pelagic, organic-rich black shales is not always associated with positive excursions (e.g., Menegatti et al., 1998). Instead, changes in carbon flux between marine and terrestrial, and carbonate and organic matter may influence the carbon isotope record (e.g., Weissert et al., 1998; Erba et al., 1999).

Published Valanginian δ^{13}C records characteristically show relatively low, consistent values throughout the early part of the stage and then a rapid shift to more positive values in the mid-Valanginian. The positive event is followed by a return to pre-excursion values in the latest Valanginian and Early Hauterivian. This trend is well known from Tethyan bulk marine carbonate records (e.g., Lini et al., 1992; Channell et al., 1993; Weissert et al., 1998; Duchamp-Alphonse et al., 2007) and has also been observed in a marine carbonate (belemnite) record from Russia (Price and Mutterlose, 2004), a marine carbonate (oyster) record from Argentina (Aguirre-Urreta et al., 2008) and in a fossilised wood record from the Crimea (Gröcke et al., 2005), which until now, was the only terrestrial record of this event. Furthermore, the Valanginian positive carbon isotope event has never been recorded from a geographically and temporally coeval terrestrial–marine record.

In recent years, several authors have attempted to correlate marine and terrestrial carbon isotope records using data from biostratigraphically constrained successions (e.g., Hesselbo et al., 2003, 2007; Pearce et al., 2005; Van de Schootbrugge et al., 2005; Nunn et al., 2009). Such comparisons can theoretically be used to evaluate the relationship between oceanic and atmospheric carbon isotope reservoirs. However, given the provinciality experienced by ammonites during the Cretaceous, precise correlation of the data from geographically different successions is problematic. The obvious solution is to compare marine and terrestrial records where the material occurs within the same geological succession at the same time. However, such successions are rare and few studies of this nature have been published for the Cretaceous.

This study presents new Ryazanian–Valanginian δ^{13}C data from two shallow marine successions in the Russian Arctic. Fossil wood and belemnites were sampled from the Boyarka River, Siberia and additional belemnites were sampled from the Izhma River, Russia. The carbon isotope data derived from the sampled material provide: (1) the first Boreal terrestrial δ^{13}C record of the Valanginian, and (2) the first truly coeval terrestrial–marine δ^{13}C record of the Valanginian. Such records can be used to confirm whether the Valanginian positive carbon isotope excursion is recorded in the Boreal terrestrial realm (where it has never before been observed), and furthermore, whether the isotope event is geologically simultaneous in the oceanic and atmospheric carbon reservoirs, as well as in the Tethyan and Boreal realms. Ultimately, these records will determine whether the observed isotopic perturbations affected the total exchangeable carbon reservoir as part of a global δ^{13}C event.

2. Study sites and sampling

2.1. Boyarka River (northern-central Siberia)

The section of the Boyarka River investigated here is situated approximately 240 km southwest of the Siberian town Khatanga, at a present-day latitude of ~70°N (Fig. 1). Five Lower Cretaceous outcrops – the key outcrops identified in the study of Shulgina et al. (1994) – were visited along a 15 km stretch of the Boyarka River. The outcrops are typically low river-side cliffs cut almost perpendicular to strike. The Cretaceous clastic succession is very well exposed at the specified outcrops but unfortunately, the exposure between these outcrops is poor and consequently, there are some gaps in the stratigraphic record. The composite Boyarka River succession is c. 300 m thick and ranges in age from the Ryazanian *kochi* Russian ammonite Zone to the Late Valanginian *bojarkensis* ammonite Zone (Fig. 2). The arrangement of the individual outcrops into one composite section, together with the biostratigraphy, is based on the work of Golbert et al. (1981) and Shulgina et al. (1994).

During the Early Cretaceous, shallow marine conditions prevailed in the Boyarka River region (at a palaeolatitude of ~70°N; Smith et al., 1994), depositing a relatively thick succession of sandstones, siltstones and clays. The Ryazanian sediments are dominated by grey silty-clays with occasional concretions and limestone bands. Above this, the basal Valanginian sediments are composed of green sandstones, with occasional thin clay beds. The sandstones display some bioturbation and cross-bedding, and also contain concretions. Clays become more dominant in the Upper Valanginian and are often mottled red from iron-staining. The uppermost Valanginian sediments comprise pale grey/green sandstones and clayey-sands. Towards the top of the succession, large but rare, isolated concretions are found. Thin clay layers containing small concretions are also found at relatively regular intervals within the *bojarkensis* Zone sediments. Fauna characteristic of marine conditions, such as belemnites and ammonites, are present throughout the succession. In addition, discrete fossilised wood fragments are also common, thus indicating a possible nearby terrestrial source from which land plants have been washed into the shallow marine environment. Belemnites of the Boreal Realm genera *Acroteuthis*, *Cylindroteuthis*, *Lagonibelus* and *Pachyteuthis* were collected from 64 horizons. Pieces of fossilised wood, which range in appearance from disseminated debris to branches <5 cm in diameter, were collected from 150 horizons. Whenever possible, multiple specimens were collected from each horizon.

2.2. Izhma River (northern Russia)

The Izhma River is a tributary of the Pechora River. It lies west of the sub-Arctic Ural Mountains at a present-day latitude of ~64°N (Fig. 1). The part of the river examined here is situated approximately 100 km north of the towns of Ukhta and Sosnogorsk. Seven Lower Cretaceous outcrops were identified along a ~90 km stretch of the river. The outcrops are in the form of low river cuttings and foreshores, and are generally well exposed. The composite Lower Ryazanian (*Pseudocraspedites* and *Surites* Zone; Fig. 2) to Upper Valanginian (*bidichotomus* Zone) succession is c. 62 m thick. The compilation of the complete section is derived from the work of Mesezhnikov et al. (1979), whilst the biostratigraphy is based on that of Bodylevsky (1963), Mesezhnikov et al. (1979) and Baraboshkin (2007).

Like the Boyarka River, the Lower Cretaceous Izhma River deposits (laid down at a palaeolatitude of ~60°N; Smith et al., 1994) are composed of shallow marine clastics. The Ryazanian sediments are composed of sandstones, silty-sandstones and clays, and contain small phosphatic nodules/concretions. These sediments become more iron-rich towards the Ryazanian–Valanginian boundary, which is marked by a red claystone bed of ~30 cm thickness. The Lower Valanginian grey silty-clays become sandier into the Upper Valanginian and large fossil-bearing carbonate concretions are found in several horizons. A relatively thick sandstone bed dominates the Upper Valanginian part of the succession and is surrounded by poorly exposed clays. Belemnites and ammonites are present throughout the succession. The Boreal Realm belemnite genera present in the Boyarka River succession (*Acroteuthis*, *Cylindroteuthis*, *Lagonibelus* and *Pachyteuthis*) are also present here and were collected bed-by-bed from 42 different horizons. Fossilised wood fragments were identified in the lowermost part of the Izhma River succession but they were not collected because they are rare and poorly preserved.

Author's personal copy

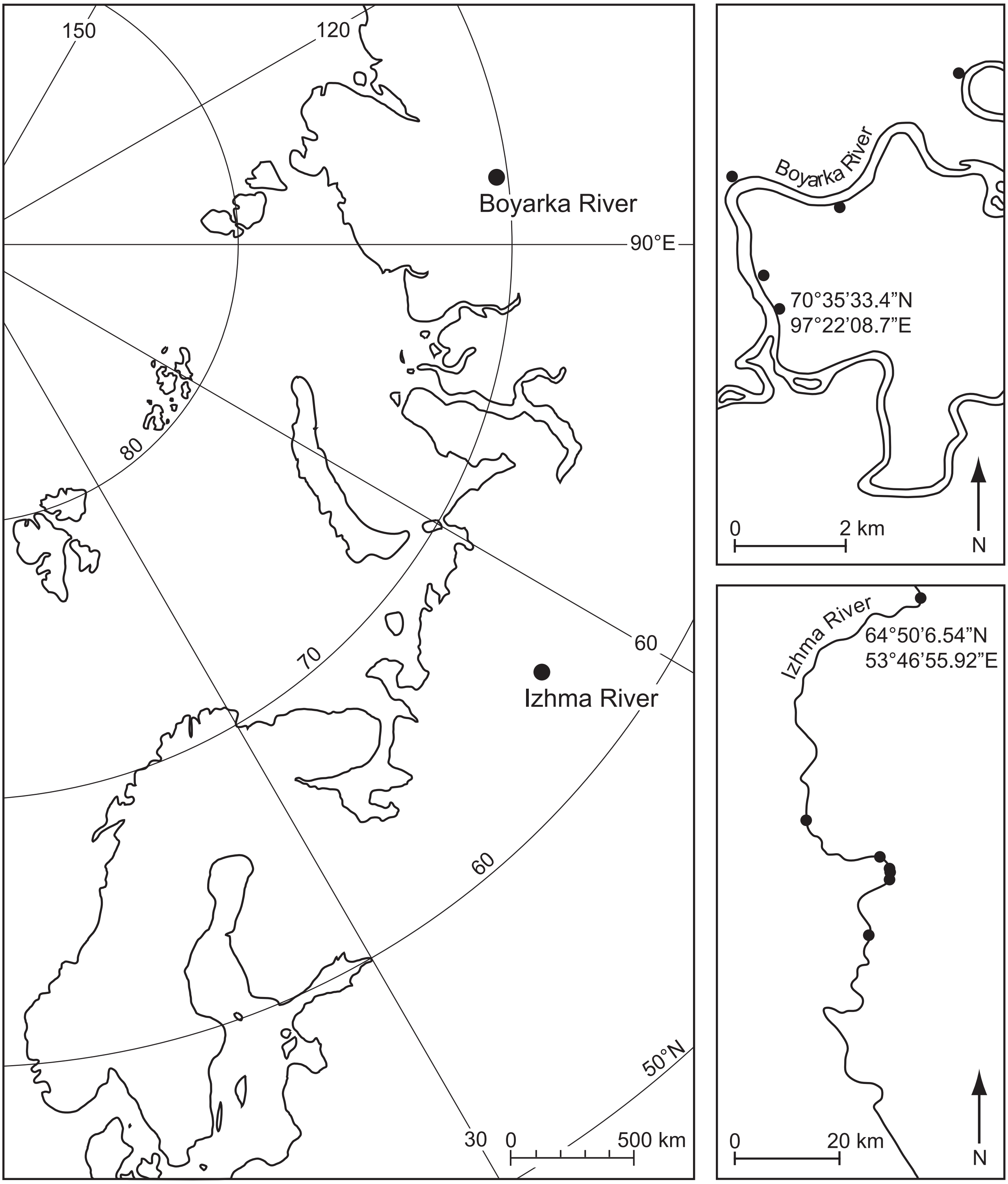

Fig. 1. Locality map showing the sections studied in northern Russia. Insert maps show the locations studied along each river (against one of which are the co-ordinates required for location).

2.3. *Stratigraphic comparisons*

The Early Cretaceous Boyarka River and Izhma River successions are different with respect to their stratigraphic thickness. The clastic sediments of the Boyarka River succession (*kochi*–*bojarkensis* zones) are approximately 320 m thick, whilst those of the Izhma River (*Pseudocraspedites* and *Surites*–*bidichotomus* zones) are just 62 m thick. This disparity is caused by the different depositional conditions prevailing at each site. The Boyarka River sediments were deposited in very shallow marine conditions, close to a major clastic source, as demonstrated by the abundance of terrestrial wood in the succession. The resulting deposits are therefore fairly expanded. Conversely, the Izhma River sediments were deposited under more open marine conditions on a broad, stable basement high (Zonenshain et al., 1990). The consequence of which is the formation of a relatively thin sedimentary cover punctuated by depositional

Author's personal copy

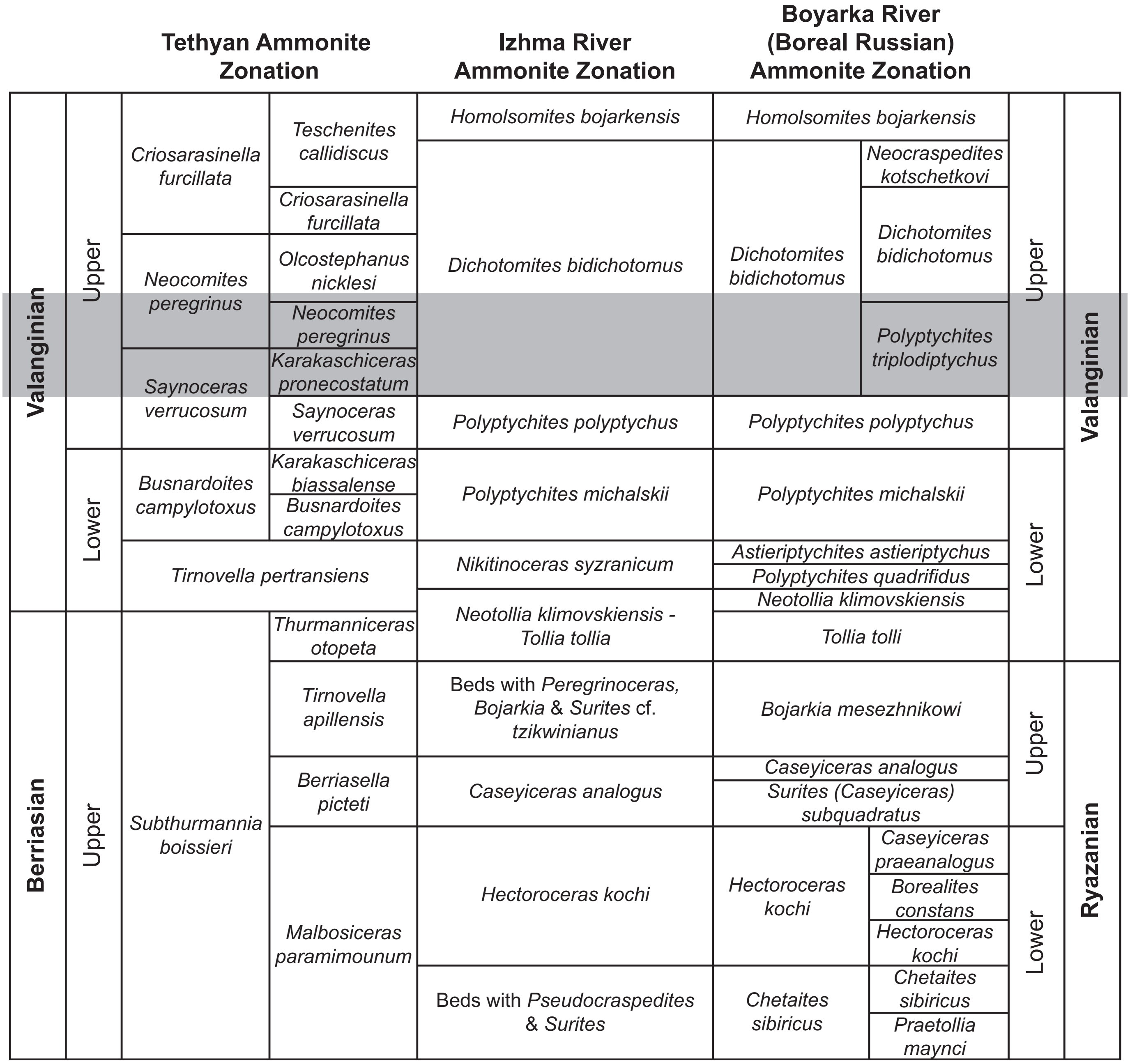

		Tethyan Ammonite Zonation		Izhma River Ammonite Zonation	Boyarka River (Boreal Russian) Ammonite Zonation			
Valanginian	Upper	*Criosarasinella furcillata*	*Teschenites callidiscus*	*Homolsomites bojarkensis*	*Homolsomites bojarkensis*		Upper	**Valanginian**
				Dichotomites bidichotomus	*Dichotomites bidichotomus*	*Neocraspedites kotschetkovi*		
			Criosarasinella furcillata			*Dichotomites bidichotomus*		
		Neocomites peregrinus	*Olcostephanus nicklesi*					
			Neocomites peregrinus			*Polyptychites triplodiptychus*		
		Saynoceras verrucosum	*Karakaschiceras pronecostatum*					
			Saynoceras verrucosum	*Polyptychites polyptychus*	*Polyptychites polyptychus*			
	Lower	*Busnardoites campylotoxus*	*Karakaschiceras biassalense*	*Polyptychites michalskii*	*Polyptychites michalskii*		Lower	
			Busnardoites campylotoxus					
		Tirnovella pertransiens		*Nikitinoceras syzranicum*	*Astieriptychites astieriptychus*			
					Polyptychites quadrifidus			
				Neotollia klimovskiensis - Tollia tollia	*Neotollia klimovskiensis*			
Berriasian	Upper	*Subthurmannia boissieri*	*Thurmanniceras otopeta*		*Tollia tolli*			
			Tirnovella apillensis	Beds with *Peregrinoceras, Bojarkia* & *Surites* cf. *tzikwinianus*	*Bojarkia mesezhnikowi*		Upper	**Ryazanian**
			Berriasella picteti	*Caseyiceras analogus*	*Caseyiceras analogus*			
					Surites (Caseyiceras) subquadratus			
			Malbosiceras paramimounum	*Hectoroceras kochi*	*Hectoroceras kochi*	*Caseyiceras praeanalogus*	Lower	
						Borealites constans		
						Hectoroceras kochi		
				Beds with *Pseudocraspedites* & *Surites*	*Chetaites sibiricus*	*Chetaites sibiricus*		
						Praetollia maynci		

Fig. 2. Biostratigraphic correlation of the Early Cretaceous Tethyan (Reboulet et al., 2009), Izhma River (Baraboshkin, 2007, this paper) and Boyarka River (Baraboshkin, 2004a, 2007) ammonite schemes. Correlations are based on Ogg et al. (2008), Gradstein et al. (2004) and Baraboshkin (2004a,b, 2005, 2007). The grey box indicates the approximate position of the Valanginian positive excursion maximum.

hiatuses, because even minor sea-level fluctuations could lead to submarine erosion or subaerial exposure (Sahagian et al., 1996). Despite the contrasting lithostratigraphy of the Boyarka and Izhma River successions, a comparative δ^{13}C investigation is still possible, even though the record of short-term fluctuations in the δ^{13}C signal may be slightly distorted (e.g., if minor oscillations occur during a hiatus they may not be recorded, or if they occur during a period of rapid deposition they may appear expanded). Long term and significant shifts however, should still be identifiable and providing the biostratigraphy of each of the successions is reliable and well resolved, any temporal effects relating to the variable lithostratigraphy, should be minimised.

Both of the successions were dated using the Boreal Russian ammonite biostratigraphy. Field observations were compared with the published logs of Golbert et al. (1981) and Mesezhnikov et al. (1979) for the Boyarka River and Izhma River respectively, with particular emphasis placed on the identification and correlation of relatively distinct marker beds. The biostratigraphy assigned on the basis of comparisons with previously published work, was then verified and refined using abundant and well-preserved ammonites collected from each succession (that are currently stored at the Moscow State University, Russia). Fig. 2 illustrates some minor differences in Boreal ammonite biozonation between the Boyarka and Izhma River successions. Such differences exist as a result of the highly provincial nature of ammonites during the Cretaceous Period, with minor differences in the biostratigraphic schemes determined by the relative occurrence and abundance of locally dominant taxa. Cretaceous provinciality prevents the development

Author's personal copy

of a truly global biostratigraphic scheme for this time interval, however it is possible to correlate different schemes that are characteristic of distinct palaeogeographical regions (e.g., Boreal vs. Tethyan ammonites; Fig. 2). The correlation of Boreal–Tethyan biostratigraphy has been attempted by a number of authors (e.g., Sey and Kalacheva, 1999; Zakharov et al., 1997; Gradstein et al., 2004; Baraboshkin, 2007), typically by identifying localities with a mixed Tethyan–Boreal fauna or alternatively by employing additional techniques such as chemostratigraphy or magnetostratigraphy. Whilst such correlations are often difficult to establish and seldom perfect, they nevertheless provide an extremely valuable tool for investigating the timing of potentially global geological events, such as the Valanginian $\delta^{13}C$ excursion.

3. Methods

In order to assess the typical preservation of the belemnite rostra representative specimens were examined through carbonate staining, cathodoluminescence (CL) and backscattered scanning electron microscopy (BSEM). The specimens were cut perpendicular to the long axis and two cross-sections (one thin, one thick) were prepared. The polished thin sections were examined under a CITL CL MK3A Luminoscope at the Camborne School of Mines (CSM), UK. The thin sections were placed in a vacuum sealed specimen chamber under an electron gun emitting a cathode ray (gun current ~450 μA, gun voltage ~10 kV) and photographed. The same thin sections were subsequently etched with dilute HCl, immersed in a mixture of alizarin red-S and potassium ferricyanide and finally, were stained with alizarin red-S to intensify the colour differentiation (following the carbonate staining technique of Dickson (1966)). The stained thin sections were then quick-dried before being photographed under a low-powered binocular microscope. The polished thick sections were placed uncoated in a JEOL 5600 scanning electron microscope (SEM) at the University of Plymouth, UK. The samples were photographed under low vacuum conditions using a backscattered electron detector (accelerating voltage 15 kV, spot size 38) to show the atomic number contrast on the polished surface.

Belemnites were prepared for isotopic and geochemical analyses by first removing the exterior of the rostrum, the apical region, the alveolus, and significant areas of cracks/fractures using a circular saw and lapping wheel, because such regions are likely to have been effected by diagenesis. The remaining calcite was fragmented, washed in pure water and dried in a clean environment. Well-preserved, translucent fragments were selected using a binocular microscope and then powdered using an agate pestle and mortar. The resultant sample was divided for stable isotope and trace element analyses. The sub-samples taken for trace element (Fe and Mn) analysis were digested in 20% HNO_3 and analyzed by Inductively Coupled Plasma–Atomic Emission Spectrometer (ICP–AES) using a Perkin Elmer Optima 3300RL ICP–AES system (with autosampler) at the NERC ICP facility, Royal Holloway, UK. Carbon isotope data were generated on a VG Optima mass spectrometer with a Multiprep Automated Carbonate System at the University of Plymouth, UK and on a VG Optima mass spectrometer following vacuum extraction of the CO_2 at the NERC Isotope Geosciences Laboratory (NIGL), Keyworth, UK. Oxygen isotope data were also generated but are not reported here as they will form the basis of a separate publication. Replicate analyses were run to ensure reproducibility, which was generally $<0.1‰$ for samples and standard materials. Carbon isotope ratios are given in δ notation reported in per mille (‰) relative to the International Standards Vienna Pee Dee Belemnite (VPDB) by comparison with laboratory standards calibrated using NBS standards (Table 1).

A representative group of fossil wood samples was photographed under a JEOL 5600 SEM. The 184 fossil wood samples taken from the Boyarka River succession were analyzed for organic carbon isotope ratios. Where possible, samples were divided to allow a portion of the material to be archived. The analyzed samples were treated with 5% HCl to remove any carbonate and then rinsed with deionised water before being oven-dried and powdered with an agate pestle and mortar. The homogenised samples were weighed and placed in tin capsules for combustion in an elemental analyzer. The resultant gas was purified and passed through a SIRA II Series 2 dual-inlet isotope-ratio mass spectrometer at McMaster University, Canada. Carbon isotope ratios are given in δ notation reported in per mille (‰) relative to the International Standards Vienna Pee Dee Belemnite (VPDB) by comparison with laboratory standards calibrated using NBS-21. Analytical reproducibility using this method was generally $<0.1‰$ for samples and standard materials (Table 2).

4. Results

The vast majority of the belemnites collected from the Boyarka and Izhma River successions were composed of honey-coloured, translucent calcite, with primary concentric banding. Fe- and Mn-rich calcite, characteristic of diagenetically altered material, was identified through BSEM, CL and carbonate staining. Diagenesis was most common around the rostrum margin, along the apical canal, and surrounding well-developed fractures. Such areas were removed prior to isotopic and geochemical sampling because even subtle alteration can destroy the primary isotopic/geochemical signal. Belemnite preservation was further assessed via trace element analysis. This was conducted on every specimen analyzed. Fe and Mn values for the Boyarka River belemnites were 3–52 ppm (mean 9 ppm) and 2–149 ppm (mean 11 ppm) respectively (Fig. 3). The Izhma River Fe values were 8–312 ppm (mean 30 ppm) and the Mn values were 2–105 ppm (mean 11 ppm) (Fig. 3). Belemnites with high concentrations of Fe (>150 ppm) and Mn (>100 ppm) were considered to have undergone post-depositional alteration and were consequently excluded from further analysis (e.g., Price and Mutterlose, 2004; Nunn et al., 2009). Carbon isotope ratios were measured from the well-preserved belemnites. Ryazanian–Valanginian values of -1.07 to $+4.24‰$ for the Boyarka River and -0.95 to $+4.05‰$ for the Izhma River were recorded. The range of values is the same for each succession (within analytical error) and furthermore, the same overall $\delta^{13}C_{carb}$ trend is observed in both successions (Fig. 4). Relatively low carbon isotope values occur in the Ryazanian and Early Valanginian, followed by a shift towards the most positive values in the *michalskii–polyptychus* zones. The shift in values associated with the positive carbon isotope excursion is ~4‰. High values persist throughout the Late Valanginian but a return towards pre-excursion values occurs in the latest Valanginian *bojarkensis* Zone.

The Boyarka River macroscopic wood samples were examined under a microscope and the state of preservation determined. Identification of the wood to generic or specific level was not undertaken. Of the 173 samples examined, 39 were identified as charcoal, 77 as charcoal–coal and 57 as coal, on the basis of distinctive plant cells and structures, which are clearly visible in the charcoal samples but completely homogenised in the coal. Representative samples were imaged using an SEM (Fig. 5). The range of preservation did not have a significant impact on the overall long-term $\delta^{13}C_{wood}$ curve (as previously demonstrated by Hesselbo et al. (2003) and Gröcke et al. (2005)). The $\delta^{13}C_{wood}$ values range between -27.20 and $-21.21‰$ for the Ryazanian–Valanginian succession (Fig. 4). The amount of scatter present in the Boyarka River wood data is comparable with that in previously published

Author's personal copy

Table 1
Carbon isotope and trace element data of belemnite specimens analyzed from the Early Cretaceous Boyarka River and Izhma River successions.

Sample ID	Location	Height (m)	Ammonite zone	Genus	$\delta^{13}C_{carb}$ (‰)	Fe (ppm)	Mn (ppm)
KH16; 0.90	Boyarka River	1.90	*H. kochi*	*Cylindroteuthis*	−0.95	9	6
KH16; 1.10	Boyarka River	2.10	*H. kochi*	*Cylindroteuthis*	0.50	8	9
KH16; 1.15	Boyarka River	2.15	*H. kochi*	*Cylindroteuthis*	−0.54	8	6
KH16; 1.25	Boyarka River	2.25	*H. kochi*	*Cylindroteuthis*	0.55	9	9
KH16; 1.30	Boyarka River	2.30	*H. kochi*	?*Cylindroteuthis*	0.49	6	6
KH16; 1.50 A	Boyarka River	2.50	*H. kochi*	?*Cylindroteuthis*	−0.57	5	7
KH16; 1.50 B	Boyarka River	2.50	*H. kochi*	?*Cylindroteuthis*	0.03	5	15
KH16; 1.60 1	Boyarka River	2.60	*H. kochi*	Indet.	−0.30	4	13
KH16; 1.60 2	Boyarka River	2.60	*H. kochi*	Indet.	−0.32	4	14
KH16; 1.65 i	Boyarka River	2.65	*H. kochi*	?*Cylindroteuthis*	0.52	4	5
KH16; 1.65 ii	Boyarka River	2.65	*H. kochi*	?*Cylindroteuthis*	0.45	5	5
KH16; 1.70 A	Boyarka River	2.70	*H. kochi*	*Cylindroteuthis*	−0.51	3	16
KH16; 2.40	Boyarka River	3.40	*H. kochi*	*Cylindroteuthis*	−0.96	7	7
KH16; 2.45 A	Boyarka River	3.45	*H. kochi*	*Lagonibelus*	−0.29	6	13
KH16; 2.60 A	Boyarka River	3.60	*H. kochi*	*Cylindroteuthis*	0.07	4	10
KH16; 2.65 A	Boyarka River	3.65	*H. kochi*	*Cylindroteuthis*	−0.03	6	6
KH16; 2.75	Boyarka River	3.75	*H. kochi*	*Cylindroteuthis*	−0.11	3	6
KH16; 2.80 A i	Boyarka River	3.80	*H. kochi*	*Cylindroteuthis*	0.41	11	20
KH16; 2.80 A ii	Boyarka River	3.80	*H. kochi*	*Cylindroteuthis*	0.14	9	20
KH16; 2.80 B	Boyarka River	3.80	*H. kochi*	*Cylindroteuthis*	0.28	9	6
KH16; 2.85 A	Boyarka River	3.85	*H. kochi*	*Acroteuthis*	−0.74	9	4
KH16; 2.85 B	Boyarka River	3.85	*H. kochi*	?*Cylindroteuthis*	0.11	8	6
KH16; 2.95 A	Boyarka River	3.95	*H. kochi*	*Cylindroteuthis*	0.31	14	31
KH16; 2.95 B	Boyarka River	3.95	*H. kochi*	*Cylindroteuthis*	0.28	9	4
KH16; 3.00 i	Boyarka River	4.00	*H. kochi*	*Cylindroteuthis*	0.84	9	16
KH16; 3.00 ii	Boyarka River	4.00	*H. kochi*	*Cylindroteuthis*	0.87	10	16
KH16; 3.50 A	Boyarka River	4.50	*S. subquadratus–C. analogus*	*Acroteuthis*	−0.44	8	5
KH16; 3.50 B	Boyarka River	4.50	*S. subquadratus–C. analogus*	?*Cylindroteuthis*	−0.53	8	5
KH16; 3.80	Boyarka River	4.80	*S. subquadratus–C. analogus*	?*Cylindroteuthis*	0.94	9	3
KH16; 4.10 i	Boyarka River	5.10	*S. subquadratus–C. analogus*	*Cylindroteuthis*	−1.07	9	5
KH16; 4.10 ii	Boyarka River	5.10	*S. subquadratus–C. analogus*	*Cylindroteuthis*	−1.04	8	6
KH17a; -1.00 i	Boyarka River	20.50	*S. subquadratus–C. analogus*	*Cylindroteuthis*	−0.25	9	4
KH17a; -1.00 ii	Boyarka River	20.50	*S. subquadratus–C. analogus*	*Cylindroteuthis*	−0.25	10	5
KH17a; -0.50 A	Boyarka River	21.00	*B. mesezhnikovi*	*Cylindroteuthis*	0.39	8	2
KH17a; L	Boyarka River	21.50	*B. mesezhnikovi*	*Cylindroteuthis*	0.39	9	4
KH17b; 1.25	Boyarka River	22.75	*B. mesezhnikovi*	*Cylindroteuthis*	1.19	9	4
KH17b; 1.55 A	Boyarka River	23.05	*B. mesezhnikovi*	*Cylindroteuthis*	0.58	8	2
KH17b; 1.55 B	Boyarka River	23.05	*B. mesezhnikovi*	*Cylindroteuthis*	0.06	10	4
KH17b; 1.75 i	Boyarka River	23.25	*B. mesezhnikovi*	?*Cylindroteuthis*	0.85	8	3
KH17b; 1.75 ii	Boyarka River	23.25	*B. mesezhnikovi*	?*Cylindroteuthis*	0.92	8	3
KH17b; 1.95	Boyarka River	23.45	*B. mesezhnikovi*	*Lagonibelus*	0.09	10	4
KH17c; 0.50	Boyarka River	24.00	*B. mesezhnikovi*	*Cylindroteuthis*	0.73	8	4
KH17c; 1.00	Boyarka River	24.50	*B. mesezhnikovi*	*Cylindroteuthis*	0.86	8	3
KH17c; 1.50	Boyarka River	25.00	*B. mesezhnikovi*	*Cylindroteuthis*	−0.17	11	12
KH17c; 2.75 1	Boyarka River	26.25	*B. mesezhnikovi*	*Cylindroteuthis*	−0.37	8	4
KH17c; 2.75 2	Boyarka River	26.25	*B. mesezhnikovi*	*Cylindroteuthis*	−0.11	9	4
KH17c; 3.40	Boyarka River	26.90	*B. mesezhnikovi*	*Acroteuthis*	1.34	10	5
KH13; 2.30	Boyarka River	56.80	*N. klimovskiensis*	*Pachyteuthis*	−0.06	20	18
KH13; 3.05 1	Boyarka River	57.55	*N. klimovskiensis*	*Acroteuthis*	0.11	7	6
KH13; 3.05 2	Boyarka River	57.55	*N. klimovskiensis*	*Acroteuthis*	0.43	11	7
KH13; 3.35 A i	Boyarka River	57.85	*N. klimovskiensis*	*Pachyteuthis*	1.25	6	6
KH13; 3.35 A ii	Boyarka River	57.85	*N. klimovskiensis*	*Pachyteuthis*	1.56	5	5
KH13; 3.45 1	Boyarka River	57.95	*N. klimovskiensis*	*Acroteuthis*	0.69	9	8
KH13; 3.45 2	Boyarka River	57.95	*N. klimovskiensis*	*Acroteuthis*	0.60	7	12
KH13; T5	Boyarka River	58.50	*N. klimovskiensis*	*Acroteuthis*	1.30	8	9
KH13; 4.35	Boyarka River	58.85	*N. klimovskiensis*	*Acroteuthis*	0.26	10	8
KH18; 2.85	Boyarka River	140.35	*N. klimovskiensis*	Indet.	−0.01	9	23
KH18; 7.10	Boyarka River	144.60	*P. michalskii–P. polyptychus*	*Pachyteuthis*	−0.25	9	5
KH18; 10.50 i	Boyarka River	148.00	*P. michalskii–P. polyptychus*	*Acroteuthis*	−0.11	16	12
KH18; 10.50 ii	Boyarka River	148.00	*P. michalskii–P. polyptychus*	*Acroteuthis*	−0.80	16	11
KH18; 10.90	Boyarka River	148.40	*P. michalskii–P. polyptychus*	?*Cylindroteuthis*	0.95	9	9
KH18; 11.20	Boyarka River	148.70	*P. michalskii–P. polyptychus*	Indet.	1.32	13	14
KH18; 27.00	Boyarka River	164.50	*P. michalskii–P. polyptychus*	*Lagonibelus*	1.20	10	4
KH1-4b; -20.00 A	Boyarka River	250.50	*P. michalskii–P. polyptychus*	*Acroteuthis*	2.73	13	8
KH1-4b; -20.00 B	Boyarka River	250.50	*P. michalskii–P. polyptychus*	*Acroteuthis*	2.96	5	5
KH1-4; 4.00 A	Boyarka River	262.00	*D. bidichotomus*	?*Cylindroteuthis*	4.24	15	3
KH1-4; 4.10 i	Boyarka River	262.10	*D. bidichotomus*	*Cylindroteuthis*	3.43	13	9
KH1-4; 4.10 ii	Boyarka River	262.10	*D. bidichotomus*	*Cylindroteuthis*	3.30	10	10
KH1-4; 4.30	Boyarka River	262.30	*D. bidichotomus*	*Cylindroteuthis*	2.35	8	13
KH1-4; 4.40 1	Boyarka River	262.40	*D. bidichotomus*	*Pachyteuthis*	2.36	11	8
KH1-4; 4.40 2	Boyarka River	262.40	*D. bidichotomus*	*Pachyteuthis*	1.68	17	8
KH1-4; 10.70	Boyarka River	268.70	*D. bidichotomus*	?*Pachytuethis*	3.61	9	13
KH1-4; 21.00	Boyarka River	279.00	*D. bidichotomus*	*Acroteuthis*	1.33	10	39
KH1-4; 21.40	Boyarka River	279.40	*H. bojarkensis*	*Cylindroteuthis*	1.00	13	39

Author's personal copy

Table 1 (*continued*).

Sample ID	Location	Height (m)	Ammonite zone	Genus	$\delta^{13}C_{carb}$ (‰)	Fe (ppm)	Mn (ppm)
KH1-4; 32.30 A[a]	Boyarka River	290.30	*H. bojarkensis*	*Cylindroteuthis*	1.52	52	149
KH1-4; 32.30 B	Boyarka River	290.30	*H. bojarkensis*	*Cylindroteuthis*	1.65	6	10
KH1-4; 47.10	Boyarka River	305.10	*H. bojarkensis*	*Cylindroteuthis*	1.72	7	12
KH1-4; 61.10	Boyarka River	319.10	*H. bojarkensis*	*Cylindroteuthis*	1.13	13	10
PC4; A	Izhma River	0.00	*Pseudocraspedites* and *Surites*	*Pachyteuthis*	−0.23	21	4
PC4; B	Izhma River	0.00	*Pseudocraspedites* and *Surites*	*Lagonibelus*	0.33	56	9
PC7.a1 Ai	Izhma River	16.70	*S. tzikwinianus–N. klimovskiensis*	*Pachyteuthis*	0.30	20	7
PC7.a1 Aii	Izhma River	16.70	*S. tzikwinianus–N. klimovskiensis*	*Pachyteuthis*	0.64	19	6
PC7.a1 B	Izhma River	16.70	*S. tzikwinianus–N. klimovskiensis*	Indet.	−0.02	27	5
PC7.a2 A	Izhma River	16.80	*S. tzikwinianus–N. klimovskiensis*	*Acroteuthis*	−0.59	19	6
PC7.a2 B	Izhma River	16.80	*S. tzikwinianus–N. klimovskiensis*	*Acroteuthis*	−0.28	19	9
PC7.b1 Ai	Izhma River	16.90	*S. tzikwinianus–N. klimovskiensis*	*Pachyteuthis*	0.10	17	4
PC7.b1 Aii	Izhma River	16.90	*S. tzikwinianus–N. klimovskiensis*	*Pachyteuthis*	−0.09	18	4
PC7.b1 B	Izhma River	16.90	*S. tzikwinianus–N. klimovskiensis*	*Pachyteuthis*	−0.64	18	5
PC7.c1	Izhma River	17.30	*S. tzikwinianus–N. klimovskiensis*	Indet.	−0.55	17	3
PC7.c2 i	Izhma River	18.00	*S. tzikwinianus–N. klimovskiensis*	*Pachyteuthis*	−0.95	17	8
PC7.c2 ii	Izhma River	18.00	*S. tzikwinianus–N. klimovskiensis*	*Pachyteuthis*	−0.57	20	7
PC7.c4 A	Izhma River	19.50	*S. tzikwinianus–N. klimovskiensis*	*Pachyteuthis*	−0.75	19	3
PC7.c4 B	Izhma River	19.50	*S. tzikwinianus–N. klimovskiensis*	*Pachyteuthis*	0.10	19	3
PC7.c6	Izhma River	19.80	*S. tzikwinianus–N. klimovskiensis*	Indet.	−0.18	13	10
PC7.c5	Izhma River	20.00	*S. tzikwinianus–N. klimovskiensis*	*Acroteuthis*	0.66	20	10
PC7.c7 i	Izhma River	21.20	*S. tzikwinianus–N. klimovskiensis*	*Pachyteuthis*	0.39	9	4
PC7.c7 ii	Izhma River	21.20	*S. tzikwinianus–N. klimovskiensis*	*Pachyteuthis*	0.73	9	4
PC7.c12[a]	Izhma River	22.30	*S. tzikwinianus–N. klimovskiensis*	Indet.	0.64	312	105
PC7.c10[a]	Izhma River	22.70	*S. tzikwinianus–N. klimovskiensis*	*?Pachyteuthis*	−0.36	274	76
PC9a	Izhma River	25.40	*N. syzranicum–P. michalskii*	*Acroteuthis*	−0.73	9	5
PC9; G1	Izhma River	26.40	*N. syzranicum–P. michalskii*	*Acroteuthis*	−0.01	58	22
PC9; G2 A	Izhma River	26.90	*N. syzranicum–P. michalskii*	*Acroteuthis*	0.24	99	26
PC9; G2 B i	Izhma River	26.90	*N. syzranicum–P. michalskii*	Indet.	0.08	36	17
PC9; G2 B ii	Izhma River	26.90	*N. syzranicum–P. michalskii*	Indet.	0.19	49	22
PC9; G3	Izhma River	27.40	*N. syzranicum–P. michalskii*	Indet.	0.16	9	4
PC9; G4	Izhma River	27.90	*N. syzranicum–P. michalskii*	Indet.	0.22	9	2
PC9; G5	Izhma River	28.40	*N. syzranicum–P. michalskii*	*Pachyteuthis*	0.32	17	20
PC9; G6	Izhma River	28.90	*N. syzranicum–P. michalskii*	*Acroteuthis*	−0.20	106	34
PC9; G7 i	Izhma River	29.40	*N. syzranicum–P. michalskii*	*Acroteuthis*	−0.34	12	9
PC9; G7 ii	Izhma River	29.40	*N. syzranicum–P. michalskii*	*Acroteuthis*	−0.68	48	27
PC9; G8	Izhma River	29.90	*N. syzranicum–P. michalskii*	*Acroteuthis*	0.91	14	9
PC9; G10	Izhma River	30.90	*N. syzranicum–P. michalskii*	*Acroteuthis*	1.61	41	21
PC9; G12 A	Izhma River	31.90	*P. polyptychus*	Indet.	3.32	10	8
PC9; G12 B	Izhma River	31.90	*P. polyptychus*	Indet.	4.05	9	5
PC9; G14 Ai	Izhma River	32.90	*P. polyptychus*	*Pachyteuthis*	0.59	34	26
PC9; G14 Aii	Izhma River	32.90	*P. polyptychus*	*Pachyteuthis*	0.62	44	29
PC9; G14 B	Izhma River	32.90	*P. polyptychus*	*Pachyteuthis*	2.29	12	7
PC9; G14a	Izhma River	33.40	*P. polyptychus*	*Pachyteuthis*	1.50	9	2
PC9; G15	Izhma River	34.40	*P. polyptychus*	Indet.	2.20	26	23
PC9; G17 i	Izhma River	35.40	*P. polyptychus*	*Pachyteuthis*	1.37	10	7
PC9; G17 ii	Izhma River	35.40	*P. polyptychus*	*Pachyteuthis*	1.45	9	7
PC9; G18 A	Izhma River	35.90	*P. polyptychus*	*Pachyteuthis*	1.28	9	5
PC9; G18 B	Izhma River	35.90	*P. polyptychus*	*Acroteuthis*	2.02	9	4
PC9; G19	Izhma River	36.40	*P. polyptychus*	*?Cylindroteuthis*	1.52	11	4
PC9; G20 Ai	Izhma River	36.70	*P. polyptychus*	*Acroteuthis*	0.90	8	2
PC9; G20 Aii	Izhma River	36.70	*P. polyptychus*	*Acroteuthis*	1.19	8	2
PC9; G20 B	Izhma River	36.70	*P. polyptychus*	*?Pachyteuthis*	1.45	10	4
PC9; G21	Izhma River	37.00	*P. polyptychus*	Indet.	2.12	8	2
PC9; G24	Izhma River	38.90	*P. polyptychus*	*Acroteuthis*	0.80	8	5
PC9; G25 Ai	Izhma River	39.40	*P. polyptychus*	Indet.	0.85	9	6
PC9; G25 Aii	Izhma River	39.40	*P. polyptychus*	Indet.	1.01	9	6
PC9; G25 B	Izhma River	39.40	*P. polyptychus*	Indet.	1.35	9	3
PC5; A	Izhma River	44.40	*D. bidichotomus*	*Pachyteuthis*	1.44	17	3
PC5; B	Izhma River	44.40	*D. bidichotomus*	*Pachyteuthis*	1.32	18	3
PC5; C	Izhma River	44.40	*D. bidichotomus*	*Pachyteuthis*	1.83	16	3
PC6.3 Ai	Izhma River	50.70	*D. bidichotomus*	*Acroteuthis*	1.60	20	16
PC6.3 Aii	Izhma River	50.70	*D. bidichotomus*	*Acroteuthis*	1.62	19	19
PC6.3 B	Izhma River	50.70	*D. bidichotomus*	Indet.	1.88	19	6
PC6.4	Izhma River	52.40	*D. bidichotomus*	*?Pachyteuthis*	1.91	28	15
PC6.5	Izhma River	56.10	*D. bidichotomus*	*Pachyteuthis*	1.53	19	4
PC6.6	Izhma River	60.10	*D. bidichotomus*	*Acroteuthis*	2.67	16	16

[a] Belemnites deemed diagenetically altered and therefore excluded from further analysis.

studies of organic carbon isotopes (e.g., Gröcke et al., 1999, 2005; Robinson and Hesselbo, 2004). The most negative $\delta^{13}C_{wood}$ values occur during the Ryazanian and Early Valanginian (*kochi–klimovskiensis* zones) and range between −27.20 and −23.74‰ (mean −24.93‰). The most positive values occur in the Valanginian *bidichotomus* Zone and are coincident with the most positive values in the Boyarka River $\delta^{13}C_{carb}$ record. *Bidichotomus* Zone $\delta^{13}C_{wood}$ values were −25.56 to −21.21‰ (mean −23.68‰).

Author's personal copy

Table 2
Carbon isotope data of fossil wood fragments from the Early Cretaceous Boyarka River succession.

Sample ID	Height (m)	Ammonite zone	Preservation	$\delta^{13}C_{wood}$ (‰)
KH16; -0.25	0.75	*H. kochi*	Charcoal	−24.03
KH16; 0.90	1.90	*H. kochi*	Charcoal–coal	−24.29
KH16; 1.00 A	2.00	*H. kochi*	Charcoal–coal	−25.08
KH16; 1.00 B	2.00	*H. kochi*	Charcoal–coal	−24.78
KH16; 1.10	2.10	*H. kochi*	Charcoal–coal	−26.98
KH16; 1.60	2.60	*H. kochi*	Charcoal–coal	−24.53
KH16; 1.70	2.70	*H. kochi*	Charcoal–coal	−23.81
KH16; 1.85	2.85	*H. kochi*	Coal	−24.33
KH16; 2.10	3.10	*H. kochi*	Coal	−23.77
KH16; 2.50	3.50	*H. kochi*	Charcoal–coal	−25.43
KH16; 3.50	4.50	*S. subquadratus–C. analogus*	Charcoal–coal	−25.46
KH16; 3.80	4.80	*S. subquadratus–C. analogus*	Coal	−24.95
KH17a; 0.25 B	21.75	*B. mesezhnikovi*	Charcoal	−26.20
KH17c; 2.25 A	25.75	*B. mesezhnikovi*	Charcoal–coal	−24.71
KH17c; 2.25 B	25.75	*B. mesezhnikovi*	Charcoal–coal	−24.43
KH17c; 2.25 C	25.75	*B. mesezhnikovi*	Charcoal	−26.72
KH17c; 2.50	26.00	*B. mesezhnikovi*	Coal	−24.88
KH17c; 2.90	26.40	*B. mesezhnikovi*	Coal	−23.74
KH13; 1.30	55.80	*N. klimovskiensis*	Charcoal	−24.45
KH13; 1.50	56.00	*N. klimovskiensis*	Charcoal	−26.62
KH13; 1.70	56.20	*N. klimovskiensis*	Charcoal	−25.30
KH13; 2.05	56.55	*N. klimovskiensis*	Charcoal	−25.28
KH13; 2.40	56.90	*N. klimovskiensis*	Charcoal	−24.30
KH13; 2.60	57.10	*N. klimovskiensis*	Charcoal	−24.87
KH13; 3.20	57.70	*N. klimovskiensis*	Charcoal	−26.22
KH13; 3.30	57.80	*N. klimovskiensis*	Charcoal	−24.39
KH13; 3.90	58.40	*N. klimovskiensis*	Charcoal–coal	−26.42
KH13; 4.45 A	58.95	*N. klimovskiensis*	Charcoal–coal	−24.72
KH13; 4.45 B	58.95	*N. klimovskiensis*	Charcoal–coal	−24.33
KH13; 4.45 C	58.95	*N. klimovskiensis*	Charcoal	−25.06
KH13; 5.25 A	59.75	*N. klimovskiensis*	Charcoal	−24.33
KH13; 5.40	59.90	*N. klimovskiensis*	Charcoal–coal	−27.20
KH13; 5.60	60.10	*N. klimovskiensis*	Coal	−24.31
KH13; 6.10	60.60	*N. klimovskiensis*	Charcoal–coal	−24.50
KH13; 6.30	60.80	*N. klimovskiensis*	Charcoal–coal	−24.40
KH13; 7.90	62.40	*N. klimovskiensis*	Coal	−25.25
KH13; 8.90 A	63.40	*N. klimovskiensis*	Charcoal	−23.86
KH13; 8.90 B	63.40	*N. klimovskiensis*	Charcoal	−24.00
KH13; 15.60 A	70.10	*N. klimovskiensis*	Coal	−24.65
KH13; 15.60 B	70.10	*N. klimovskiensis*	Coal	−24.74
KH18; 0.60	138.10	*N. klimovskiensis*	Charcoal–coal	−25.19
KH18; 1.75	139.25	*N. klimovskiensis*	Charcoal–coal	−24.98
KH18; 1.80	139.30	*N. klimovskiensis*	Charcoal–coal	−25.30
KH18; 2.30	139.80	*N. klimovskiensis*	Coal	−24.90
KH18; 2.80	140.30	*N. klimovskiensis*	Charcoal–coal	−25.12
KH18; 5.45	142.95	*N. klimovskiensis*	Charcoal–coal	−24.38
KH18; 5.85	143.35	*N. klimovskiensis*	Charcoal–coal	−23.20
KH18; 6.30 A	143.80	*P. michalskii–P. polyptychus*	Charcoal	−23.31
KH18; 6.30 B	143.80	*P. michalskii–P. polyptychus*	Coal	−23.70
KH18; 6.30 C	143.80	*P. michalskii–P. polyptychus*	Charcoal	−24.13
KH18; 6.60	144.10	*P. michalskii–P. polyptychus*	Charcoal–coal	−25.20
KH18; 8.40	145.90	*P. michalskii–P. polyptychus*	Charcoal	−24.32
KH18; 8.55	146.05	*P. michalskii–P. polyptychus*	Charcoal–coal	−23.78
KH18; 8.65 A	146.15	*P. michalskii–P. polyptychus*	Charcoal	−24.11
KH18; 8.65 B	146.15	*P. michalskii–P. polyptychus*	Charcoal–coal	−24.98
KH18; 10.00	147.50	*P. michalskii–P. polyptychus*	Charcoal–coal	−24.55
KH1-4b; -20.05	250.45	*P. michalskii–P. polyptychus*	Charcoal	−23.15
KH1-4b; -20.00	250.50	*P. michalskii–P. polyptychus*	Charcoal	−23.96
KH1-4b; -16.60	253.90	*D. bidichotomus*	Coal	−23.17
KH1-4b; -15.50	255.00	*D. bidichotomus*	Charcoal–coal	−23.85
KH1-4; -1.10	256.90	*D. bidichotomus*	Charcoal	−23.47
KH1-4; -0.80 A	257.20	*D. bidichotomus*	Charcoal–coal	−23.92
KH1-4; -0.80 B	257.20	*D. bidichotomus*	Charcoal–coal	−23.35
KH1-4b; -13.15	257.35	*D. bidichotomus*	Charcoal–coal	−22.55
KH1-4; -0.60	257.40	*D. bidichotomus*	Charcoal–coal	−22.83
KH1-4; -0.40	257.60	*D. bidichotomus*	Charcoal–coal	−25.16
KH1-4; -0.30	257.70	*D. bidichotomus*	Charcoal–coal	−24.21
KH1-4; 0.05	258.05	*D. bidichotomus*	Charcoal–coal	−23.06
KH1-4; 0.90	258.90	*D. bidichotomus*	Coal	−24.90
KH1-4; 1.30	259.30	*D. bidichotomus*	Charcoal–coal	−22.71
KH1-4; 1.70 A	259.70	*D. bidichotomus*	Coal	−22.91
KH1-4; 1.70 B	259.70	*D. bidichotomus*	Charcoal	−22.75
KH1-4; 2.00	260.00	*D. bidichotomus*	Coal	−22.00
KH1-4; 2.20	260.20	*D. bidichotomus*	Charcoal–coal	−23.24

Author's personal copy

Table 2 (*continued*).

Sample ID	Height (m)	Ammonite zone	Preservation	$\delta^{13}C_{wood}$ (‰)
KH1-4; 2.35	260.35	*D. bidichotomus*	Charcoal–coal	−22.99
KH1-4; 2.75	260.75	*D. bidichotomus*	Charcoal	−22.82
KH1-4; 2.80	260.80	*D. bidichotomus*	Charcoal–coal	−23.81
KH1-4; 3.25 A	261.25	*D. bidichotomus*	Charcoal–coal	−23.85
KH1-4; 3.25 B	261.25	*D. bidichotomus*	Charcoal–coal	−22.73
KH1-4; 3.30	261.30	*D. bidichotomus*	Charcoal	−22.85
KH1-4; 3.40	261.40	*D. bidichotomus*	Charcoal–coal	−23.58
KH1-4b; -9.00	261.50	*D. bidichotomus*	Charcoal	−22.76
KH1-4; 3.60 A	261.60	*D. bidichotomus*	Charcoal	−22.83
KH1-4; 3.60 B	261.60	*D. bidichotomus*	Charcoal	−24.23
KH1-4b; -8.80 A	261.70	*D. bidichotomus*	Charcoal–coal	−25.34
KH1-4b; -8.80 B	261.70	*D. bidichotomus*	Charcoal–coal	−23.31
KH1-4; 3.75	261.75	*D. bidichotomus*	Charcoal	−23.13
KH1-4; 3.90	261.90	*D. bidichotomus*	Coal	−23.27
KH1-4b; -8.60	261.90	*D. bidichotomus*	Charcoal–coal	−25.23
KH1-4; 4.00 A	262.00	*D. bidichotomus*	Charcoal–coal	−23.32
KH1-4; 4.00 B	262.00	*D. bidichotomus*	Charcoal	−23.95
KH1-4; 4.10	262.10	*D. bidichotomus*	Charcoal–coal	−22.38
KH1-4; 4.20	262.20	*D. bidichotomus*	Charcoal	−22.70
KH1-4; 4.40 A	262.40	*D. bidichotomus*	Charcoal	−23.85
KH1-4; 4.40 B	262.40	*D. bidichotomus*	Charcoal–coal	−21.36
KH1-4; 4.50	262.50	*D. bidichotomus*	Coal	−22.16
KH1-4b; -8.00	262.50	*D. bidichotomus*	Charcoal–coal	−23.24
KH1-4; 4.80	262.80	*D. bidichotomus*	Coal	−23.38
KH1-4; 5.10 A	263.10	*D. bidichotomus*	Charcoal–coal	−24.04
KH1-4; 5.10 B	263.10	*D. bidichotomus*	Charcoal–coal	−24.55
KH1-4; 5.20	263.20	*D. bidichotomus*	Charcoal	−25.00
KH1-4; 5.30	263.30	*D. bidichotomus*	Charcoal–coal	−24.55
KH1-4; 5.40	263.40	*D. bidichotomus*	Coal	−23.72
KH1-4; 6.00 A	264.00	*D. bidichotomus*	Charcoal–coal	−24.60
KH1-4; 6.00 B	264.00	*D. bidichotomus*	Coal	−24.49
KH1-4; 6.30 A	264.30	*D. bidichotomus*	Coal	−25.56
KH1-4; 6.30 B	264.30	*D. bidichotomus*	Charcoal–coal	−24.03
KH1-4; 6.30 C	264.30	*D. bidichotomus*	Charcoal–coal	−25.13
KH1-4; 7.00	265.00	*D. bidichotomus*	Coal	−25.05
KH1-4; 8.45	266.45	*D. bidichotomus*	Charcoal–coal	−24.34
KH1-4; 8.60	266.60	*D. bidichotomus*	Charcoal–coal	−24.37
KH1-4; 8.90 A	266.90	*D. bidichotomus*	Charcoal	−25.16
KH1-4; 8.90 B	266.90	*D. bidichotomus*	Charcoal–coal	−24.12
KH1-4; 9.30	267.30	*D. bidichotomus*	Charcoal	−23.91
KH1-4; 9.40	267.40	*D. bidichotomus*	Charcoal	−23.99
KH1-4; 9.80	267.80	*D. bidichotomus*	Charcoal–coal	−24.35
KH1-4; 11.40	269.40	*D. bidichotomus*	Coal	−24.20
KH1-4; 11.60 A	269.60	*D. bidichotomus*	Coal	−24.17
KH1-4; 11.60 B	269.60	*D. bidichotomus*	Charcoal–coal	−24.23
KH1-4; 11.80	269.80	*D. bidichotomus*	Coal	−21.21
KH1-4; 12.10	270.10	*D. bidichotomus*	Coal	−22.88
KH1-4; 12.60	270.60	*D. bidichotomus*	Coal	−21.99
KH1-4; 13.00	271.00	*D. bidichotomus*	Coal	−25.04
KH1-4; 13.20	271.20	*D. bidichotomus*	Charcoal–coal	−22.94
KH1-4; 13.60	271.60	*D. bidichotomus*	Charcoal–coal	−24.61
KH1-4; 14.50	272.50	*D. bidichotomus*	Charcoal–coal	−25.06
KH1-4; 15.20	273.20	*D. bidichotomus*	Coal	−23.29
KH1-4; 15.40 A	273.40	*D. bidichotomus*	Coal	−23.59
KH1-4; 15.40 B	273.40	*D. bidichotomus*	Coal	−23.28
KH1-4; 16.00	274.00	*D. bidichotomus*	Charcoal	−24.34
KH1-4; 17.60	275.60	*D. bidichotomus*	Coal	−23.33
KH1-4; 17.80	275.80	*D. bidichotomus*	Coal	−23.39
KH1-4; 18.20	276.20	*D. bidichotomus*	Charcoal–coal	−23.38
KH1-4; 18.50	276.50	*D. bidichotomus*	Coal	−24.21
KH1-4; 19.70	277.70	*D. bidichotomus*	Coal	−23.90
KH1-4; 19.80	277.80	*D. bidichotomus*	Coal	−22.50
KH1-4; 21.00	279.00	*D. bidichotomus*	Charcoal–coal	−25.13
KH1-4; 21.40	279.40	*H. bojarkensis*	Charcoal–coal	−25.39
KH1-4; 21.60 A	279.60	*H. bojarkensis*	Coal	−22.75
KH1-4; 21.60 B	279.60	*H. bojarkensis*	Coal	−23.57
KH1-4; 22.60	280.60	*H. bojarkensis*	Charcoal–coal	−25.56
KH1-4; 23.80	281.80	*H. bojarkensis*	Coal	−24.68
KH1-4; 24.30	282.30	*H. bojarkensis*	Coal	−23.59
KH1-4; 25.80	283.80	*H. bojarkensis*	Charcoal–coal	−23.91
KH1-4; 26.80	284.80	*H. bojarkensis*	Coal	−24.85
KH1-4; 26.90	284.90	*H. bojarkensis*	Coal	−24.91
KH1-4; 27.30	285.30	*H. bojarkensis*	Charcoal–coal	−23.77
KH1-4; 27.90 A	285.90	*H. bojarkensis*	Charcoal–coal	−24.99

(*continued on next page*)

Author's personal copy

Table 2 (*continued*).

Sample ID	Height (m)	Ammonite zone	Preservation	$\delta^{13}C_{wood}$ (‰)
KH1-4; 27.90 B	285.90	*H. bojarkensis*	Charcoal–coal	−23.19
KH1-4; 28.15	286.15	*H. bojarkensis*	Coal	−23.92
KH1-4; 28.70	286.70	*H. bojarkensis*	Charcoal–coal	−23.33
KH1-4; 30.00	288.00	*H. bojarkensis*	Coal	−23.02
KH1-4; 30.70	288.70	*H. bojarkensis*	Charcoal–coal	−23.81
KH1-4; 31.90	289.90	*H. bojarkensis*	Coal	−23.63
KH1-4; 32.10	290.10	*H. bojarkensis*	Charcoal–coal	−25.70
KH1-4; 32.30	290.30	*H. bojarkensis*	Charcoal–coal	−23.43
KH1-4; 35.70	293.70	*H. bojarkensis*	Coal	−23.91
KH1-4; 41.30	299.30	*H. bojarkensis*	Coal	−23.15
KH1-4; 41.90	299.90	*H. bojarkensis*	Coal	−23.97
KH1-4; 42.00	300.00	*H. bojarkensis*	Coal	−23.55
KH1-4; 42.30	300.30	*H. bojarkensis*	Coal	−24.03
KH1-4; 43.10	301.10	*H. bojarkensis*	Charcoal	−23.00
KH1-4; 43.50	301.50	*H. bojarkensis*	Coal	−24.27
KH1-4; 47.10 A	305.10	*H. bojarkensis*	Coal	−23.25
KH1-4; 47.10 B	305.10	*H. bojarkensis*	Coal	−23.76
KH1-4; 49.90	307.90	*H. bojarkensis*	Coal	−23.54
KH1-4; 52.70	310.70	*H. bojarkensis*	Charcoal–coal	−22.62
KH1-4; 54.00	312.00	*H. bojarkensis*	Charcoal–coal	−23.39
KH1-4; 59.30	317.30	*H. bojarkensis*	Coal	−24.67
KH1-4; 61.40	319.40	*H. bojarkensis*	Charcoal	−23.99
KH1-4; 61.60	319.60	*H. bojarkensis*	Coal	−23.12
KH1-4; 62.10	320.10	*H. bojarkensis*	Coal	−24.68
KH1-4; 64.00	322.00	*H. bojarkensis*	Charcoal–coal	−24.39

5. Discussion

5.1. *Understanding the ocean–atmosphere system*

Cretaceous marine and terrestrial records have been compared in a number of recently published studies (e.g., Ando et al., 2003; Robinson and Hesselbo, 2004; Ando and Kakegawa, 2007). Such studies typically compare marine and terrestrial records from geographically different successions, which has obvious implications in terms of precise biostratigraphic correlation. This issue is overcome here by investigating a geological succession that contains both marine carbonate (e.g., belemnites) and terrestrial organic matter (e.g., wood). The Boyarka River $\delta^{13}C_{wood}$ record displays some scatter, which can be attributed to both real environmental variability and to the sampling strategy (i.e., different floral components from different plant species were inevitably analyzed). The coeval $\delta^{13}C_{carb}$ record is also relatively 'noisy'. For example, the belemnite data show a variability of approximately 2.5‰ from one horizon at the peak of the Valanginian positive carbon isotope excursion. Such variability is consistent with other published belemnite records (e.g., Van de Schootbrugge et al., 2000; Price and Mutterlose, 2004) and may be related to short-term environmental fluctuations, to different species occupying different habitats, or to differences in biological fractionation (McArthur et al., 2007). By comparison, published bulk rock $\delta^{13}C$ curves for this interval (e.g., Lini et al., 1992; Channell et al., 1993; Weissert et al., 1998) are relatively smooth. This is the result of integrating different biogenic components, which will average out natural variability in habitat, vital effects, time and preservation (Nunn et al., 2009). The scatter observed in the Russian $\delta^{13}C_{wood}$ and $\delta^{13}C_{carb}$ records, is therefore an unavoidable consequence of analysing individual specimens (a plant or a belemnite respectively), rather than well homogenised material (bulk carbonate). As such, the scatter represents real and natural variability, meaning that broad, long-term $\delta^{13}C$ trends can still be analyzed with confidence.

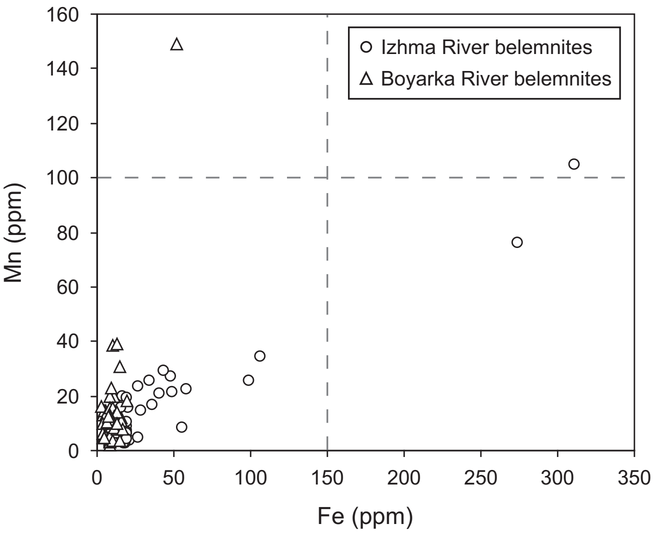

Fig. 3. Cross plot of belemnite Fe and Mn concentrations. The dashed lines mark the cut-off values for well-preserved samples.

The Early Cretaceous Boyarka River $\delta^{13}C_{wood}$ and $\delta^{13}C_{carb}$ records show the same long-term trend, with relatively negative values in the *kochi–klimovskiensis* ammonite zones, a shift towards more positive values in the *michalskii–polyptychus* zones, an excursion maximum in the *bidichotomus* Zone, and finally, a return towards pre-excursion values in the *bojarkensis* Zone (Fig. 4). There may however be a slight offset between the two records with regards to the timing of the excursion because the initiation of the positive shift in the *michalskii–polyptychus* zones is recorded slightly earlier in the wood record than it is in the belemnite record. This could be linked to a difference in carbon uptake between the continent and the ocean at this time, but more likely, this is a consequence of the limited sample recovery from this interval. Overall, the initiation, peak and decay of the Valanginian positive carbon isotope excursion appear to be broadly synchronous in both the marine and terrestrial $\delta^{13}C$ records. This confirms that the ocean–atmosphere system was strongly linked at this time and that the positive $\delta^{13}C$ excursion affected the total exchangeable carbon reservoir.

The observed offset between the Russian, Ryazanian–Valanginian $\delta^{13}C_{wood}$ and $\delta^{13}C_{carb}$ data ($\Delta\delta^{13}C$) is approximately 25‰, which is comparable with other published Mesozoic records. Nunn et al. (2009) for example, recorded an offset of ~25.5‰ in their coeval

Author's personal copy

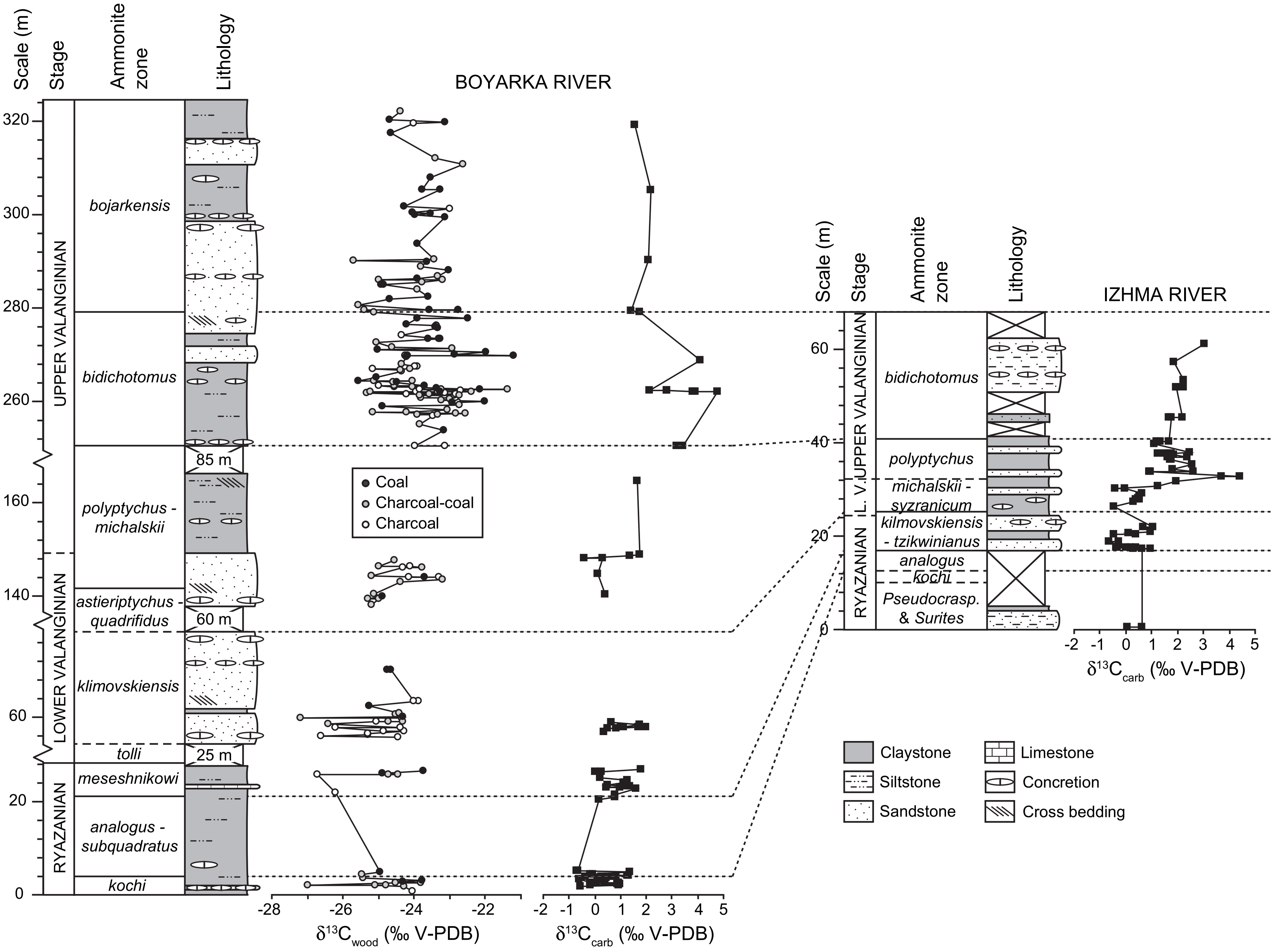

Fig. 4. Correlation of the $\delta^{13}C_{carb}$ and $\delta^{13}C_{wood}$ data from the Ryazanian–Hauterivian Boyarka River and Izhma River successions. The Boreal Russian ammonite zonation is given.

Author's personal copy

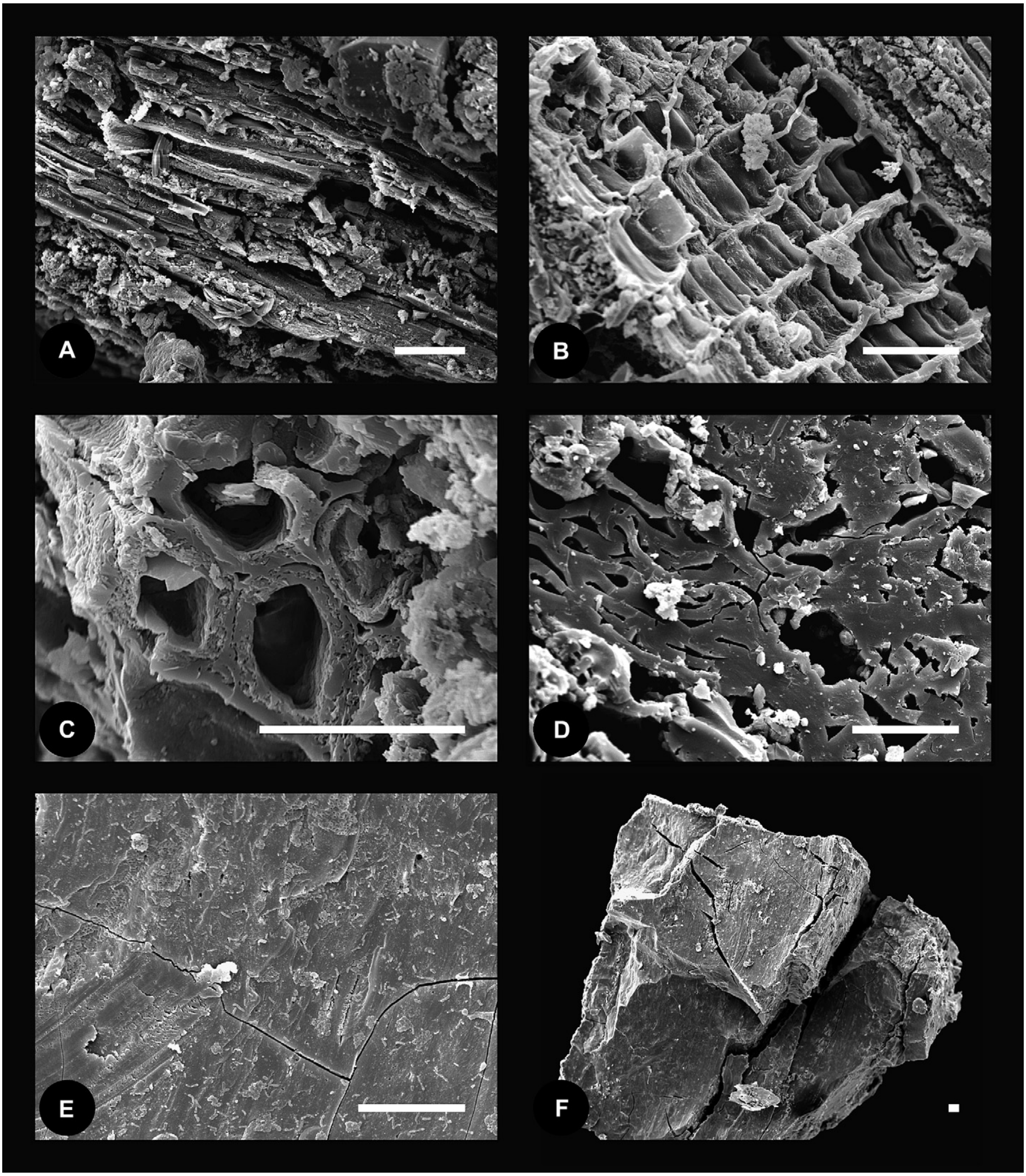

Fig. 5. Scanning electron microscope images of fossilised wood fragments from the Boyarka River, Siberia. Note the different states of preservation: charcoal (A–C), charcoal–coal (D) and coal (E, F). Distinctive plant cells and structures are clearly visible in the charcoal but such structures have been completely homogenised in the coal. All scale bars represent 20 μm.

$\delta^{13}C_{org}$–$\delta^{13}C_{belemnite}$ record for the Callovian–Kimmeridgian interval at Staffin Bay in Scotland. Interestingly however, the offset observed by Gröcke et al. (2005) for their Valanginian–Hauterivian Crimean $\delta^{13}C_{plant}$ record and a Tethyan bulk carbonate record based on data from Lini et al. (1992) and Channell et al. (1993) was slightly lower than that observed in this study, at between 22.4 and 24.6‰. This discrepancy may in part be related to a slight difference in carbonate values – a consequence of comparing belemnites with bulk rock

Author's personal copy

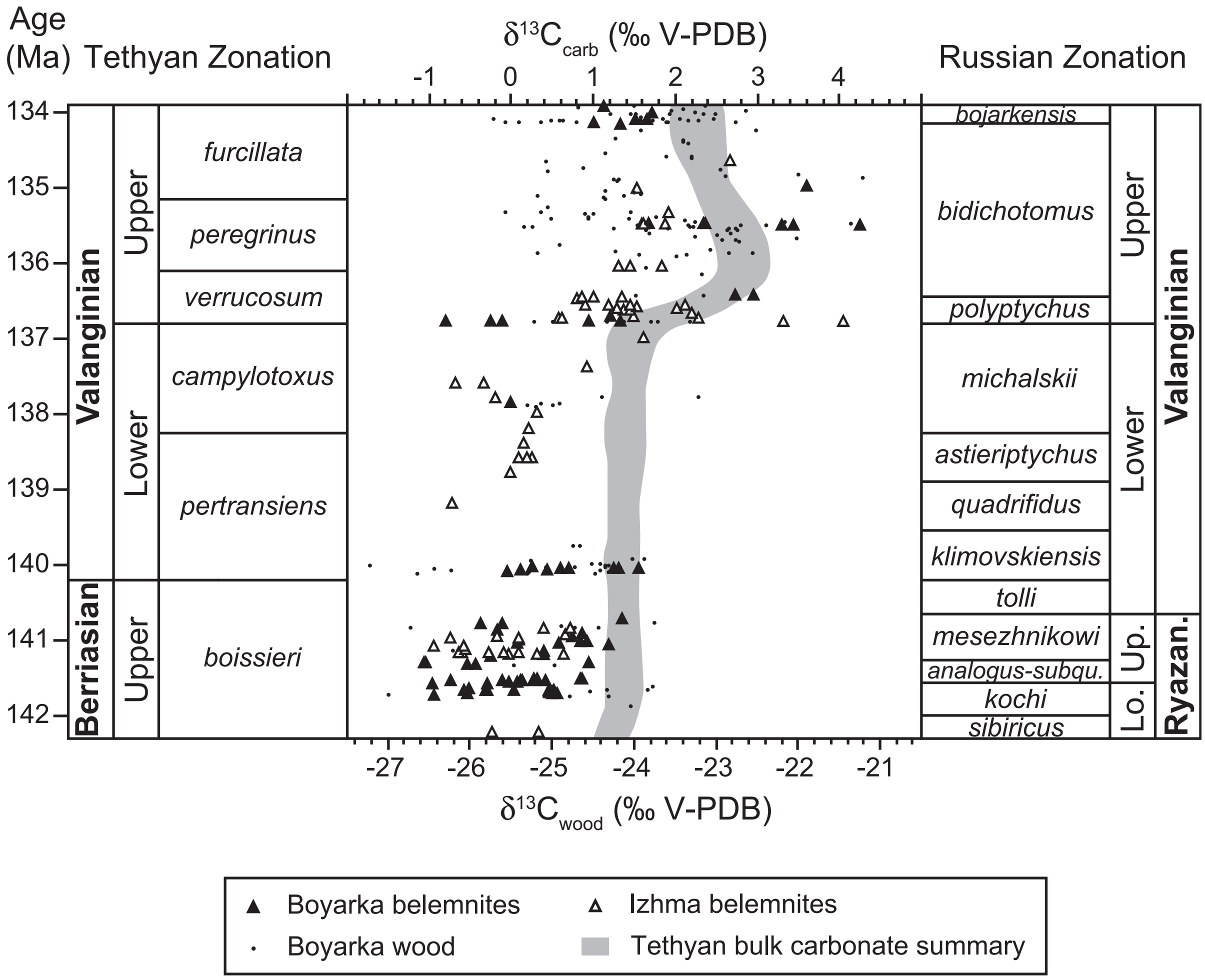

Fig. 6. Composite record of Early Cretaceous δ^{13}C data for the Boyarka River, Izhma River and published Tethyan successions. The Tethyan bulk δ^{13}C curve is based on data from Breggia, Capriolo, Polaveno, Pusiano and Val del Mis (Lini et al., 1992; Channell et al., 1993; Weissert et al., 1998). The compilation was produced by calculating the numerical age of each sample by assuming a constant sedimentation rate during each ammonite zone.

data – but primarily, it appears to be caused by the more positive $\delta^{13}C_{org}$ values in the Crimean succession, where the most positive Late Valanginian $\delta^{13}C_{org}$ value is −18.17‰, compared with −21.21‰ in Siberia (a 3‰ difference). The reason for this difference is unclear but is likely to be related to plant type, or to local influences on carbon isotope discrimination in plants, such as temperature or moisture availability.

5.2. *The Valanginian positive carbon isotope excursion: global correlations*

Published marine carbonate δ^{13}C records for the Early Cretaceous have been constructed primarily from successions in the Tethyan region. The overall pattern described from such data is one of decreasing δ^{13}C values across the Jurassic–Cretaceous boundary, relatively stable δ^{13}C values in the earliest Cretaceous, then a rapid mid- to Late Valanginian positive excursion (starting around the Tethyan *campylotoxus–verrucosum* zone boundary or time-equivalent) followed by a return towards pre-excursion values in the latest Valanginian and Early Hauterivian (e.g., Lini et al., 1992; Channell et al., 1993; Weissert et al., 1998; McArthur et al., 2007; Duchamp-Alphonse et al., 2007). Overall, the Izhma River and Boyarka River records appear to be consistent with this trend. The Izhma River δ^{13}C curve (Fig. 4) records fairly constant values for the Ryazanian to Early Valanginian interval, after which, a positive carbon isotope excursion occurs, with the initiation at the *michalskii–polyptychus* zonal boundary. The most positive δ^{13}C values are recorded in the Late Valanginian *polyptychus* Zone, although very positive values persist throughout the *bidichotomus* Zone as well. No definitive return to pre-excursion values is observed in this succession, strongly suggesting that the excursion is terminated either in the later part of the *bidichotomus* Zone or in the subsequent *bojarkensis* Zone. The Boyarka River data (Fig. 4) also record a distinct and rapid positive carbon isotope excursion in both the belemnite and wood records. Here the excursion begins in the *michalskii–polyptychus* zones, however, it should be noted that the positive shift appears to start slightly earlier in the wood record than it does in the belemnite record, probably as a result of the limited sample recovery from this interval. The Boyarka River excursion maximum occurs within the *bidichotomus* Zone in both the marine and terrestrial records, and a decline in δ^{13}C values is observed in the latest Valanginian *bojarkensis* Zone. On the whole, the Boyarka and Izhma River carbon isotope data (both marine and terrestrial) are compatable and the Russian carbon isotope trend can therefore be summarized as follows: (1) The initiation of the excursion in both the Boyarka and Izhma River successions occurs firmly within the *michalskii–polyptychus* zones – and probably near the zonal boundary – despite some uncertainty stemming from the sample recovery and biostratigraphy (e.g., since the exact placement of the *michalskii–polyptychus* boundary in the Boyarka

Author's personal copy

River succession has not been determined). (2) The excursion continues through the *polyptychus* Zone and into the *bidichotomus* Zone, where the Boyarka excursion maxima are reached. Interestingly, the most positive Izhma River values occur earlier (in the *polyptychus* Zone) but this maximum is represented by just two data points, whilst the overall *polyptychus*–*bidichotomus* trend, is one of increasingly positive values, with this increase terminated only by the top of the succession. (3) A return towards pre-excursion values is observed in the Boyarka River *bojarkensis* Zone.

The timing and duration of the positive carbon isotope event in Arctic Russia is broadly compatible with that observed in the Tethyan region (Fig. 6) although, the δ^{13}C values are typically more negative in the Russian belemnite record than in the Tethyan bulk record (with the exception of the very positive values recorded by the belemnites during the excursion itself). This systematic offset is potentially the result of the different life style of the belemnites (deeper water) compared with the plankton (near surface water) that dominate the Tethyan bulk rock record, the consequence of which, is a difference in the uptake of ^{12}C/^{13}C in carbonates because this is depth- and productivity dependent (Bodin et al., 2009). The *michalskii*–*polyptychus* boundary, near which the Izhma River and Boyarka River excursions begin, is correlatable with the start of the Tethyan excursion close to the *campylotoxus*–*verrucosum* boundary (Baraboshkin, 2005; Fig. 2). Furthermore, the increasingly positive values throughout the Boreal Russian *polyptychus*–*bidichotomus* zones, culminating in the Boyarka River *bidichotomus* peak, broadly corresponds with the timing of the Tethyan marine carbonate excursion peak in the *verrucosum*–*peregrinus* zones (Lini et al., 1992; Channell et al., 1993; Van de Schootbrugge et al., 2000; Weissert and Erba, 2004). It also corresponds with the peak of a marine carbonate excursion recorded in the Argentinean *atherstoni* ammonite Zone (Aguirre-Urreta et al., 2008) and with the peak of an organic carbon isotope excursion recorded in the Crimean *trinodosum*–*callidiscus* ammonite zones (Gröcke et al., 2005), which are correlatable with the Tethyan *verrucosum* and *peregrinus*–*furcillata* zones respectively. Any minor biostratigraphic discrepancies in the correlation between the Valanginian δ^{13}C curves are likely to be the result of problems associated with the provincial nature of ammonites, and with the correlation of the ammonite schemes with other local biostratigraphic schemes. In addition, the Boreal–Tethyan correlation (Fig. 6) required that numerical age was calculated based on an assumption of constant sedimentation during each ammonite zone. However given the expanded versus condensed nature of the Boyarka and Izhma River successions respectively this is fairly arbitrary. The age calculation may therefore also contribute to any minor discrepancies encountered. Nevertheless, given the biostratigraphic resolution currently available, it would certainly appear that the initiation, peak, and decay of the Valanginian carbon isotope excursion are consistent across the globe.

5.3. *Valanginian palaeoclimate*

Positive carbon isotope excursions are commonly linked to greenhouse conditions. Lini et al. (1992) hypothesised that the Valanginian carbon isotope event represented the first episode of greenhouse conditions during the Cretaceous period. This event has frequently been related to episodes of platform drowning in the Tethys (e.g., Lini et al., 1992; Föllmi et al., 1994; Weissert et al., 1998; Wortmann and Weissert, 2000). Van de Schootbrugge et al. (2000) however highlighted the problem with this model, which is that during the Hauterivian, at least two phases of platform drowning are not associated with positive carbon isotope excursions. Wortmann and Weissert (2000) suggested that the sea-level rise and drowning of platform carbonates corresponded instead to the initiation of more positive carbon isotope values, rather than to the most positive values themselves. According to the sea-level curve of Sahagian et al. (1996), the Valanginian positive carbon isotope excursion occurs during a period of relatively low sea-level on the Russian Platform and in Siberia. It should be noted that although the Sahagian et al. (1996) sea-level curve is contrary to the sea-level curve of Haq et al. (1987), the Valanginian section of the Sahagian et al. curve was constructed from data taken from the Boyarka River succession itself. A period of sea-level lowstand would have resulted in the partial separation of the Boreal and Tethyan Realms and could have restricted ocean circulation and enhanced ocean water stratification to promote organic carbon burial in these high latitude locations. This would be consistent with the apparent lack of extensive deep marine black shales in the Late Valanginian, which could be explained by carbon burial away from typical, mid- to low-latitude, open marine settings (Price and Mutterlose, 2004; Aguirre-Urreta et al., 2008). For example, Westermann et al. (2010) propose an alternative driving mechanism for the Valanginian δ^{13}C excursion, where the enhanced production and storage of organic carbon occurs on the continent. In addition, an increased input of nutrients resulting from the exposure and erosion of lowland areas (Brenchley et al., 1994; Gröcke et al., 1999; Price and Mutterlose, 2004) may have contributed to an increase in primary productivity and consequently could have influenced the shift towards positive carbon isotope values at this time.

The mid-Valanginian global carbon isotope event also appears to be coincident with a short-term cooling episode. Price and Mutterlose (2004) report increasing δ^{18}O values, and therefore decreasing palaeotemperatures, following the positive δ^{13}C excursion in their Valanginian Russian belemnite record. Such a fall in temperatures, could be explained by increased organic carbon burial and a drawdown of atmospheric CO_2. The concept of a Valanginian cooling event is consistent with other recently published isotope evidence for this period (e.g., Pucéat et al., 2003; Erba et al., 2004; McArthur et al., 2007) and with the presence of glendonites in several Valanginian high latitude successions (e.g., Kemper, 1987; Price and Nunn, 2010).

6. Conclusions

This paper presents δ^{13}C data from two shallow marine successions in the Boyarka River, Siberia and the Izhma River, Russia. These data comprise the first Boreal terrestrial organic δ^{13}C record of the mid-Valanginian positive carbon isotope excursion, as well as the first coeval terrestrial–marine δ^{13}C record of this event. Both the terrestrial organic δ^{13}C (wood) record and the marine carbonate δ^{13}C (belemnite) record show distinct positive carbon isotope excursions, with the initiation in the Boreal Russian *michalskii*–*polyptychus* ammonite zones, the peak in the *bidichotomus* Zone, and a return towards pre-excursion values in the latest Valanginian *bojarkensis* Zone. These zones are equivalent to the Tethyan *campylotoxus*–*verrucosum*, *verrucosum*–*furcillata* and uppermost *furcillata* ammonite zones respectively. The event is synchronous in the marine and terrestrial records from the Boyarka and Izhma Rivers and furthermore, these Boreal records are correlatable with other published carbon isotope curves from this event, for example, in Tethyan bulk marine carbonate (e.g., Lini et al., 1992; Channell et al., 1993), in Crimean wood (e.g., Gröcke et al., 2005) and in Argentinean oysters (e.g., Aguirre-Urreta et al., 2008). The occurrence of this event in the northern hemisphere, southern hemisphere and Tethys, in both the marine and terrestrial realms, confirms that the Valanginian positive carbon isotope excursion is a globally synchronous event, during which the total exchangeable carbon reservoir was affected, and as such, it can be used as a global carbon isotope marker.

Author's personal copy

Acknowledgements

This study was supported by the University of Plymouth (Ph.D. studentship to EVN), NERC (grant number OSS/305/1105to GDP), the Russian Foundation for Basic Research (grant numbers 03-05-79054k, 04-05-64503a and 07-05-00882a to EYB) and the British Federation of Women Graduates (Johnstone & Florence Stoney Studentship to EVN). We are grateful for the technical support of J. Duffett at Royal Holloway for trace element analysis, to P. Frost at the Camborne School of Mines for cathodoluminescence microscopy and to a number of people at NIGL for the belemnite isotope analysis. This paper benefited from the constructive reviews of Stéphane Bodin and an anonymous reviewer.

References

Aguirre-Urreta, M.B., Price, G.D., Ruffell, A.H., Lazo, D.G., Kalin, R.M., Ogle, N., Rawson, P.F., 2008. Southern hemisphere Early Cretaceous (Valanginian–Early Barremian) carbon and oxygen isotope curves from the Neuquén Basin, Argentina. Cretaceous Research 29, 87–99.

Ando, A., Kakegawa, T., 2007. Carbon isotope records of terrestrial organic matter and occurrence of planktonic foraminifera from the Albian stage of Hokkaido, Japan: Ocean–atmosphere delta C-13 trends and chronostratigraphic implications. Palaios 22, 417–432.

Ando, A., Kakegawa, T., Takashima, R., Saito, T., 2003. Stratigraphic carbon isotope fluctuations of detrital woody materials during the Aptian stage in Hokkaido, Japan: Comprehensive delta C-13 data from four sections of the Ashibetsu area. Journal of Asian Earth Sciences 21, 835–847.

Baraboshkin, E.J., 2004a. Lower Cretaceous Zonal standard of the Boreal Realm. Bulletin of the Moscow Society of Naturalists, Series Geology 79 (5), 44–68 (in Russian).

Baraboshkin, E.J., 2004b. Boreal–Tethyan correlation of Lower Cretaceous ammonite scales. Moscow University Geology Bulletin 59 (6), 9–20 (in Russian).

Baraboshkin, E.J., 2005. The Lower Cretaceous marine Boreal cephalopod zonal standard. In: Godet, A., Mort, H., Linder, P., Bodin, S. (Eds.), 7th International Symposium on the Cretaceous 5–9 September 2005, Scientific Program and Abstracts, pp. 43–45.

Baraboshkin, E.J., 2007. Stratigraphy and Boreal–Tethyan correlation of marine Lower Hauterivian of Russia and CIS. In: Pervushov, E.M. (Ed.), Selected Papers of the Third All-Russia Meeting 'Cretaceous System of Russia and Near Overseas: Problems of Stratigraphy and Paleogeography. Publishing House of Saratov State University, Saratov, pp. 21–35 (in Russian).

Bodin, S., Fiet, N., Godet, A., Matera, V., Westermann, S., Clément, A., Janssen, N.M.M., Stille, P., Föllmi, K.B., 2009. Early Cretaceous (late Berriasian to early Aptian) palaeoceanographic change along the northwestern Tethyan margin (Vocontian Trough, southeastern France): δ^{13}C, δ^{18}O and Sr-isotope belemnite and whole-rock records. Cretaceous Research 30, 124–1262.

Bodylevsky, V.I., 1963. The Cretaceous. In: Zoricheva, A.I., Volkov, S.N. (Eds.), Geology of the USSR, t.II, Arkhangelsk, Vologda Regions and Komi ASSR. Part 1. Geological Description. Gosgeoltekhizdat, Moscow, pp. 666–682 (in Russian).

Brenchley, P.J., Marshall, J.D., Carden, G.A.F., Robertson, D.B.R., Long, D.G.F., Meidla, T., Hints, L., Anderson, T.F., 1994. Bathymetric and isotopic evidence for a short-lived Late Ordovician glaciation in a greenhouse period. Geology 22, 295–298.

Channell, J.E.T., Erba, E., Lini, A., 1993. Magnetostratigraphic calibration of the Late Valanginian carbon isotope event in pelagic limestones from Northern Italy and Switzerland. Earth and Planetary Science Letters 118, 145–166.

Claypool, G.E., Baysinger, J.P., 1980. Analysis of organic matter in sediment cores from the Moroccan Basin, Deep Sea Drilling Project Sites 415 and 416. In: Stout, L.N., Worstell, P., Lancelot, Y., et al. (Eds.), Initial Reports of the Deep Sea Drilling Project. US Government Printing Office, Washington, DC, pp. 605–608. 50.

Courtillot, V., Jaupart, C., Manighetti, I., Tapponnier, P., Besse, J., 1999. On causal links between flood basalts and continental breakup. Earth and Planetary Science Letters 166, 177–195.

Dickson, J.A.D., 1966. Carbonate identification and genesis as revealed by staining. Journal of Sedimentary Petrology 36, 491–505.

Duchamp-Alphonse, S., Gardin, S., Fiet, N., Bartolini, A., Blamart, D., Pagel, M., 2007. Fertilization of the northwestern Tethys (Vocontian basin, SE France) during the Valanginian carbon isotope perturbation: evidence from calcareous nannofossils and trace element data. Palaeogeography, Palaeoclimatology, Palaeoecology 243, 132–151.

Erba, E., Channell, J.E.T., Claps, M., Jones, C., Larson, R., Opdyke, B., Silva, I.P., Riva, A., Salvini, G., Torricelli, S., 1999. Integrated stratigraphy of the Cismon APTICORE (Southern Alps, Italy): a 'reference section' for the Barremian–Aptian interval at low latitudes. Journal of Foraminiferal Research 29, 371–391.

Erba, E., Bartolini, A., Larson, R.L., 2004. Valanginian Weissert oceanic anoxic event. Geology 32, 149–152.

Föllmi, K.B., Weissert, H., Bisping, M., Funk, H., 1994. Phosphogenesis, carbon-isotope stratigraphy, and platform evolution along the Lower Cretaceous northern Tethyan margin. Geological Society of America Bulletin 106, 729–746.

Golbert, A.V., Bulynnikova, S.P., Grigorieva, K.N., Deviatov, V.P., Zakharov, V.A., Kazakov, A.M., Klimova, I.G., Reshetnikova, M.A., Sanin, V.Y., Turbina, A.S., 1981. Reference Section of the Neocomian of the North of Siberian Platform (Enisei–Khatanga Trough, Anabar–Katanga Depression). Geological Description, vol. 1 & 2. Trudy SNIGGIMS, Novosibirsk, 98 pp. and 134 pp. (in Russian).

Gradstein, F., Ogg, J., Smith, A., 2004. A Geologic Timescale 2004. Cambridge University Press, Cambridge, 589 pp.

Gröcke, D.R., Hesselbo, S.P., Jenkyns, H.C., 1999. Carbon-isotope composition of Lower Cretaceous fossil wood: ocean–atmosphere chemistry and relation to sea-level change. Geology 27, 155–158.

Gröcke, D.R., Price, G.D., Robinson, S.A., Baraboshkin, E.Y., Mutterlose, J., Ruffell, A.H., 2005. The Upper Valanginian (Early Cretaceous) positive carbon-isotope event recorded in terrestrial plants. Earth and Planetary Science Letters 240, 495–509.

Haq, B.U., Hardenbol, J., Vail, P.R., 1987. Chronology of fluctuating sea levels since the Triassic. Science 235, 1156–1167.

Herbin, J.P., Deroo, G., Roucache, J., 1984. Organic geochemistry of lower Cretaceous sediments from site 535, Leg 77: Florida Straits. In: Buffler, R.T., Schlager, W. (Eds.), Initial Reports of the Deep Sea Drilling Project, vol. 29. US Government Printing Office, Washington, DC, pp. 459–474.

Hesselbo, S.P., Morgans-Bell, H.S., McElwain, C., McAllister Rees, P., Robinson, S.A., Ross, C.E., 2003. Carbon-cycle perturbation in the Middle Jurassic and accompanying changes in the terrestrial paleoenvironment. Journal of Geology 111, 259–276.

Hesselbo, S.P., Jenkyns, H.C., Duarte, L.V., Oliveira, L.C.V., 2007. Carbon-isotope record of the Early Jurassic (Toarcian) Oceanic Anoxic Event from fossil wood and marine carbonate (Lusitanian Basin, Portugal). Earth & Planetary Science Letters 253, 455–470.

Kemper, E., 1987. Das Klima der Kreide-zeit. Geologisches Jahrbuch A96, 5–185 (in German).

Lini, A., Weissert, H., Erba, E., 1992. The Valanginian carbon isotope event: a first episode of greenhouse climate conditions during the Cretaceous. Terra Nova 4, 374–384.

McArthur, J.M., Janssen, N.M.M., Reboulet, S., Leng, M.J., Thirlwall, M.F., van de Schootbrugge, B., 2007. Palaeotemperatures, polar ice-volume, and isotope stratigraphy (Mg/Ca, δ^{18}O, δ^{13}C, ^{87}Sr/^{86}Sr): the Early Cretaceous (Berriasian, Valanginian, Hauterivian). Palaeogeography, Palaeoclimatology, Palaeoecology 248, 391–430.

Menegatti, A.P., Weisser, H., Brown, R.S., Tyson, R.V., Farrimond, P., Strasser, A., Caron, M., 1998. High-resolution δ^{13}C stratigraphy through the early Aptian 'Livello Selli' of the Alpine Tethys. Paleoceanography 13, 530–545.

Mesezhnikov, M.S., Golbert, A.V., Zakharov, V.A., Klimova, I.G., Shulgina, N.L., Alekseev, S.N., Bulvnnikova, S.P., Kuzina, V.I., Yakovleva, S.P., 1979. News in the stratigraphy of the Jurassic–Cretaceous boundary beds in the Pechora River Basin. In: Saks, V.N. (Ed.), The Upper Jurassic and Its Boundary with the Cretaceous. Nauku Publications, Novosibirsk, pp. 66–71 (in Russian).

Nunn, E.V., Price, G.D., Hart, M.B., Page, K.N., Leng, M.J., 2009. Isotopic signals from Callovian–Kimmeridgian (Middle–Upper Jurassic) belemnites and bulk organic carbon, Staffin Bay, Isle of Skye, Scotland. Journal of the Geological Society, London 166, 633–641.

Ogg, J.G., Ogg, G., Gradstein, F.M., 2008. The Concise Geologic Time Scale. Cambridge University Press, Cambridge, 177 pp.

Pearce, C.R., Hesselbo, S.P., Coe, A.L., 2005. The mid-Oxfordian (Late Jurassic) positive carbon-isotope excursion recognised from fossil wood in the British Isles. Palaeogeography, Palaeoclimatology, Palaeoecology 221, 343–357.

Price, G.D., Mutterlose, J., 2004. Isotopic signals from late Jurassic–early Cretaceous (Volgian–Valanginian) sub-Arctic belemnites, Yatria River, Western Siberia. Journal of the Geological Society, London 161, 959–968.

Price, G.P., Nunn, E.V., 2010. Valanginian isotope variation in glendonites and belemnites from Arctic Svalbard: Transient glacial temperatures during the Cretaceous greenhouse. Geology 38, 251–254.

Pucéat, E., Lécuyer, C., Sheppard, S.M.F., Dromart, G., Reboulet, S., Grandjean, P., 2003. Thermal evolution of Cretaceous Tethyan marine waters inferred from oxygen isotope composition of fish tooth enamels. Paleoceanography 18, PA1029. doi:10.1029/2002PA000823.

Reboulet, S., Klein, J., Barragan, R., Company, M., Gonzalez-Arreola, C., Lukeneder, A., Raisossadat, S.N., Sandoval, J., Szives, O., Tavera, J.M., Vasicek, Z., Vermeulen, J., 2009. Report on the 3rd International Meeting of the IUGS Lower Cretaceous Ammonite Working Group, the "Kilian Group" (Vienna, Austria, 15th April 2008). Cretaceous Research 30, 496–502.

Robinson, S.A., Hesselbo, S.P., 2004. Fossil-wood Carbon-isotope Stratigraphy of the Non-marine Wealden Group (Lower Cretaceous, Southern England). Journal of the Geological Society, London 161. 133–145.

Sahagian, D., Pinous, O., Olferiev, A., Zakharov, V., 1996. Eustatic curve for the Middle Jurassic–Cretaceous based on Russian platform and Siberian stratigraphy: zonal resolution. American Association of Petroleum Geologists Bulletin 80, 1433–1458.

Sey, I.I., Kalacheva, E.D., 1999. Lower Berriasian of southern Primorye (Far East Russia) and the problem of Boreal–Tethyan correlation. Palaeogeography, Palaeoclimatology, Palaeoecology 150, 49–63.

Shipboard Scientific Party, 2002. Leg 198 summary. In: Bralower, T.J., Premoli Silva, I., Malone, M.J. (Eds.), Proceedings of the Ocean Drilling Program, Initial Reports, 198. Ocean Drilling Program, College Station, TX, pp. 1–148.

Shulgina, N.I., Burdykina, M.D., Basov, V.A., Århus, N., 1994. Distribution of ammonites, foraminifera and dinoflagellate cysts in the Lower Cretaceous reference sections of the Khatanga Basin, and Boreal Valanginian biogeography. Cretaceous Research 15, 1–16.

Smith, A.G., Smith, D.G., Funnell, B.M., 1994. Atlas of Mesozoic and Cenozoic Coastlines. Cambridge University Press, Cambridge, 99 pp.

Author's personal copy

Van de Schootbrugge, G., Föllmi, K.B., Bulot, L.G., Burns, S.J., 2000. Paleoceanographic changes during the Early Cretaceous (Valanginian–Hauterivian): evidence from oxygen and carbon stable isotopes. Earth and Planetary Science Letters 181, 15–31.

Van de Schootbrugge, B., McArthur, J.M., Bailey, T.R., Rosenthal, Y., Wright, J.D., Miller, K.G., 2005. Toarcian oceanic anoxic event: an assessment of global causes using belemnite C isotope records. Paleoceanography 20, PA3008. doi:10.1029/2004PA001102.

Weissert, H., Erba, E., 2004. Volcanism, CO_2 and palaeoclimate: a Late Jurassic–Early Cretaceous carbon and oxygen isotope record. Journal of the Geological Society, London 161, 695–702.

Weissert, H., Lini, A., Föllmi, K.B., Kuhn, O., 1998. Correlation of Early Cretaceous carbon isotope stratigraphy and platform drowning events: a possible link? Palaeogeography, Palaeoclimatology, Palaeoecology 137, 189–203.

Westermann, S., Föllmi, K.B., Adatte, T., Matera, V., Schnyder, J., Fleitmann, D., Fiet, N., Ploch, I., Duchamp–Alphonse, S., 2010. The Valanginian $\delta^{13}C$ excursion may not be an expression of a global oceanic anoxic event. Earth and Planetary Scienc Letters 290, 118–131.

Wortmann, U.G., Weissert, H., 2000. Tying platform drowning to perturbations of the global carbon cycle with a $\delta^{13}C$ Org curve from the Valanginian of DSDP Site 416. Terra Nova 12, 289–294.

Zakharov, V.A., Bogomolov, Y.I., Ilyina, V.I., Konstantinov, A.G., Kurushin, N.I., Lebedeva, N.K., Meledina, S.V., Nikitenko, B.L., Sobolev, E.S., Shurygin, B.N., 1997. Boreal zonal standard and biostratigraphy of the Siberian Mesozoic. Geology and Geophysics, Siberian Branch 38, 927–956 (in Russian).

Zonenshain, L.P., Kuzmin, M.I., Natapov, L.M., 1990. Geology of the USSR: a Plate Tectonic Synthesis. American Geophysical Union, Washington DC, 242 pp.